Aus dem Institut für Neurophysiologie
der Universität zu Köln
Direktor (Kommissarische Leitung): Professor Kurt Pfannkuche

Unveiling the Proliferative and Arrhythmogenic Potential of Strontium Chloride and Potassium Carbonate in Pluripotent Stem Cells and Cardiomyocytes

Inaugural-Dissertation zur Erlangung der zahnärztlichen Doktorwürde
der Medizinischen Fakultät
der Universität zu Köln

vorgelegt von
Saheera Kumar
aus Köln

promoviert am 17. April 2026

Gedruckt mit Genehmigung der Medizinischen Fakultät der Universität zu Köln
2026

Dekan: Universitätsprofessor Dr. med. G. R. Fink
1. Gutachter: Privatdozent Dr. med. F. Nguemo
2. Gutachter: Universitätsprofessor Dr. M. Bergami

Erklärung

Ich erkläre hiermit, dass ich die vorliegende Dissertationsschrift ohne unzulässige Hilfe Dritter und ohne Benutzung anderer als der angegebenen Hilfsmittel angefertigt habe; die aus fremden Quellen direkt oder indirekt übernommenen Gedanken sind als solche kenntlich gemacht.

Bei der Auswahl und Auswertung des Materials sowie bei der Herstellung des Manuskriptes habe ich keine Unterstützungsleistungen erhalten.

Weitere Personen waren an der Erstellung der vorliegenden Arbeit nicht beteiligt. Insbesondere habe ich nicht die Hilfe einer Promotionsberaterin/eines Promotionsberaters in Anspruch genommen. Dritte haben von mir weder unmittelbar noch mittelbar geldwerte Leistungen für Arbeiten erhalten, die im Zusammenhang mit dem Inhalt der vorgelegten Dissertationsschrift stehen.

Die Dissertationsschrift wurde von mir bisher weder im Inland noch im Ausland in gleicher oder ähnlicher Form einer anderen Prüfungsbehörde vorgelegt.

Die in dieser Arbeit angegebenen Experimente der Zellproliferation mit iPSCs sind nach entsprechender Anleitung durch Herrn Privatdozent Dr. Filomain Nguemo von mir selbst ausgeführt worden. Die entsprechenden Versuche mit iPSC-abgeleiteten Kardiomyozyten wurden durch Herrn Privatdozent Dr. Filomain Nguemo durchgeführt.

Die Durchführung der Durchflusszytometrie erfolgte durch die wissenschaftliche Mitarbeiterin Frau Michelle Kamga Kapchoup, der dieser Arbeit zugrunde liegenden Datensatz der Durchflusszytometrie wurde gemeinsam mit mir auf FlowJo7 ausgewertet.
Die Messergebnisse des Mikroelektrodenarrays wurden ohne meine Mitarbeit im Institut für Neurophysiologie von Herr Jude Tsefack ermittelt, die der Polymerase-Kettenreaktion in Echtzeit von Herr Hai Zhang.

Bei der sprachlichen Überarbeitung (Grammatik, Rechtschreibung und Ausdruck) habe ich das KI-basierte Sprachmodell ChatGPT (OpenAI) ausschließlich zur sprachlichen Korrektur eingesetzt. Inhalt, Argumentation und wissenschaftliche Auswertung stammen vollständig von mir selbst.

Erklärung zur guten wissenschaftlichen Praxis:

Ich erkläre hiermit, dass ich die Ordnung zur Sicherung guter wissenschaftlicher Praxis und zum Umgang mit wissenschaftlichem Fehlverhalten (Amtliche Mitteilung der Universität zu Köln AM 132/2020) der Universität zu Köln gelesen habe und verpflichte mich hiermit, die dort genannten Vorgaben bei allen wissenschaftlichen Tätigkeiten zu beachten und umzusetzen.

Köln, den

Unterschrift: .....

Acknowledgements

First and foremost, I would like to express my sincere gratitude to Prof. Dr. Dr. Jürgen Hescheler, former Director of the Institute of Neurophysiology at the University of Cologne, for granting me access to the Institute and the opportunity to carry out this research project.

I am especially and deeply grateful to my supervisor, PD Dr. Filomain Nguemo, whose scientific expertise, patience, and insightful guidance were instrumental in the successful completion of this work. His constant encouragement and constructive feedback helped me navigate the challenges of this project.

I would also like to express my appreciation to the technical staff of the Institute of Neurophysiology, especially Mrs. Annette Köster, Mrs. Susanne Rohani, and Michelle V. Kamga Kapchoup, for their support with laboratory procedures and ensuring a well-functioning lab environment.

Lastly, I wish to thank my family and friends for their unwavering support, motivation, and belief in me throughout this academic journey and my life in general.

My sincere thanks to all

Das Leben schickt uns nur Prüfungen, die wir meistern können.

TABLE OF CONTENTS

Abbreviation

α-MHC	alpha-myosin heavy chain
β	Beta
μ	Micro sign
ASC	Adult stem cell
BVL	Federal Office of Consumer Protection and Food Safety (Bundesamt für Verbraucherschutz und Lebensmittelsicherheit)
Ctrl	Control
cDNA	Complementary DNA
CI	Cell Index
CMs	Cardiomyocyte
DMEM	Dulbecco`s modified eagle medium
DPBS	Dulbecco's phosphate-buffered saline
eGFP	IRES-flanked enhanced green fluorescent protein
EB	Embryoid body
EMA	European Medicines Agency
ESC	Embryonic stem cell
FACS	Fluorescence-activated cell sorting
hBD-3	Human β-defensin 3
hESC	Human embryonic stem cell
hiPSC	Human induced pluripotent stem cell
ICM	Inner cell mass
IL-6	Interleukin 6
IMDM	Iscove´s Modified Dulbecco´s Medium
iPSC	Induced pluripotent stem cell
iPSC-CM	IPSC derived cardiomyocyte

K_2CO_3	Potassium Carbonate
LIF	Leukemia inhibitory factor
MEF	Mouse embryonic fibroblast
mES	Murine embryonic stem cell
n	An integer, whose value can be varied
NCX	Na^+/Ca^{2+} exchanger
NEAA	Non-essential amino acids
PAC	Puromycin resistance gene N- acetyl-aminotransferase
PBS	Phosphate buffer saline
PCR	Polymerase chain reaction
PFA	Paraformaldehyde
PI	Propidium Iodide
PRAC	Pharmacovigilance Risk Assessment Committee
PSC	Pluripotent stem cell
qPCR	Quantitative PCR
qRT-PCR	Quantitative real-time PCR
RT	Room Temperature
RTCA	Real-Time Analysis Cardio Instrument
SSCS/SCCP	Scientific Committee on Consumer Safety
SEM	Standard error of the mean
SOCS3	Suppressor of cytokine signaling 3
$SrCl_2$	Strontium Chloride
TGF-β	Transforming growth factor-β
TNF-α	Tumor Necrosis Factor-α

1. Zusammenfassung

Zahlreiche Inhaltsstoffe in alltäglichen Kosmetika und Pflegeprodukten gelten als unbedenklich, obwohl ihre potenziellen toxikologischen Effekte, insbesondere im kardialen Kontext, bisher nicht ausreichend untersucht wurden. In der vorliegenden Studie wurde der Einfluss von Strontiumchlorid ($SrCl_2$) und Kaliumcarbonat (K_2CO_3), zwei in Zahnpasta eingesetzten Ionenverbindunden, auf murine induzierte pluripotente Stammzellen (iPSCs) und daraus abgeleitete Kardiomyozyten (iPSC-CMs) untersucht.

Mittels Impedanz-basierter Echtzeitmessung (xCELLigence), Durchflusszytometrie (FACS), multielektrodenbasierter Elektrophysiologie (MEA), Immunfluoreszenz und quantitativer PCR (qRT-PCR) wurden zytotoxische, elektrophysiologische und molekulare Effekte analysiert.

Die Ergebnisse zeigen, dass niedrige Konzentrationen beider Substanzen vorübergehend die iPSC-Proliferation steigerten, während höhere Konzentrationen signifikant zytotoxisch wirkten. FACS-Analysen belegten eine signifikante Zunahme toter iPSCs, insbesondere nach Exposition mit 3.15 mM $SrCl_2$ und 3.2 mM K_2CO_3. Bei iPSC-CMs zeigte das Impedanzverfahren überdies eine konzentrationsabhängige Abnahme der Zell-Viabilität und Kontraktionsaktivität, insbesondere unter höheren K_2CO_3-Konzentrationen. Diese funktionellen Verluste traten ergänzend zu den MEA-basierten elektrophysiologischen Störungen auf. Speziell $SrCl_2$ führte bei Konzentrationen > 1.6 mM zu deutlichen Änderungen der Feldpotenzialamplitude und der Schlagfrequenz. K_2CO_3 dagegen verursachte bei 3.2 mM eine ausgeprägtere Störung. Die beobachteten elektrophysiologischen Effekte sind konsistent mit bekannten Wirkmechanismen (z.B. Sr^{2+} als Ca^{2+}-Analogen; K^+-induzierte Depolarisationsblockade), konnten jedoch in dieser Studie nicht kausal nachgewiesen werden und bleiben hypothetisch. Auch auf molekularer Ebene wurden Veränderungen in der Genexpression beobachtet. $SrCl_2$ führte zu einer initialen Reduktion Kardiomyozyten-spezifischer Gene (z.B. *Mesp1, Mlc2v*), die sich teils nach 72 h wieder normalisierte. K_2CO_3 hingegen bewirkte eine anhaltende Suppression struktureller und elektrophysiologischer Marker (z.B. *Myh6, Scn5a, Kcnh2*), was auf eine stärkere Beeinträchtigung kardialer Genprogramme hindeutet.

Zusammenfassend zeigt die Studie, dass $SrCl_2$ und K_2CO_3 dosisabhängige zelluläre Effekte auf Proliferation, Viabilität, Elektrophysiologie und Genexpression entfalten. Beide Substanzen wirken zytotoxisch in höheren Konzentrationen, jedoch wahrscheinlich über unterschiedliche Mechanismen. Basierend auf Plausibilität und Literaturvergleich entfaltet $SrCl_2$ seine Wirkung vermutlich über gestörte Calcium-Signalwege, K_2CO_3 primär über Membrandepolarisation, wobei letzteres zu einem schnellen Funktionsverlust, $SrCl_2$ zu einem progressiven Funktionsabbau, führt. Die Ergebnisse unterstreichen die Relevanz iPSC- und iPSC-CM basierter *in vitro* Modelle zur Erkennung potenzieller Kardio- und Zytotoxizität auch bei scheinbar unproblematischen Inhaltsstoffen. Weitere Studien mit human Zellen,

Langzeitexpositionen sowie präklinische Validierung sind erforderlich, um das Risiko von $SrCl_2$ und K_2CO_3 im Kontext realer Anwendungsszenarien sicher beurteilen zu können.

Summary

Many consumer products are used in routine without sufficient awareness of the toxicological risks posed by certain ingredients. Strontium Chloride ($SrCl_2$) and Potassium Carbonate (K_2CO_3), both found in some toothpaste formulations, remain under-researched in terms of their cardiotoxic potential. This study aimed to systematically assess the toxicological effects of $SrCl_2$ and K_2CO_3 on murine induced pluripotent stem cells (iPSCs) and iPSC-derived cardiomyocytes (iPSC-CMs) using a multi-assay approach. We employed impedance-based real-time cell analysis (xCELLigence), multielectrode array (MEA) recordings, PI-based flow cytometry (FACS), immunocytochemistry, and quantitative real-time PCR (qRT-PCR) to evaluate cytotoxic, electrophysiological, and molecular effects across multiple time intervals and compound concentrations.

Our data shows that both compounds induced a dose-dependent biphasic response in undifferentiated iPSCs: low-dose $SrCl_2$ and K_2CO_3 exposure showed trends toward increased proliferation, followed by significant dose-dependent cytotoxic effects at higher concentrations. In iPSC-CMs, impedance-based measurements showed a concentration-dependent reduction in viability and contractile behavior, particularly under high K_2CO_3 concentrations. These findings confirm functional cytotoxicity beyond earlier instances and complement the MEA-derived electrophysiological disturbances. $SrCl_2$ exposure led to noticeable changes in both spike amplitude and frequency, suggesting calcium overload. K_2CO_3 in contrast, caused an immediate suppression of electrical activity and beating rate at higher doses, consistent with depolarization-induced electrical silencing. FACS analysis confirmed increased cell death in both treatment groups. Gene expression analysis revealed that $SrCl_2$ affected structural genes with partial recovery over 72 hours, whereas K_2CO_3 caused persistent downregulation of contractile and ion channel genes (e.g., *Scn5a, Myh6, Kcnh2*), highlighting different underlying toxicological mechanisms.

Together, these findings demonstrate that $SrCl_2$ and K_2CO_3 exert significant, concentration-dependent cardiotoxic and cytotoxic effects in murine iPSCs and iPSC-CMs via distinct ionic and molecular pathways. These results underscore the importance of evaluating even simple inorganic ingredients for their potential cardiac impact and advocate for further investigation using human-relevant models to better inform safety assessments of oral care products.

2. Introduction

2.1. The Clinical Importance of Dentifrice Components

Toothpaste primarily serves as a support to mechanical plaque removal; however, modern formulations are expected to fulfill a wide range of functions. Depending on their intended purpose, toothpastes are formulated for cavity prevention, gingivitis control, teeth whitening, or reducing hypersensitivity. Their composition (**Table 1**) typically includes key ingredients such as abrasives, detergents, and fluoride, each with a distinct role[1].

Table 1. Typical Ingredients and Proportions in Toothpaste Formulations adapted from Weber [2]

Ingredients	Examples	Proportions in %
Water	-	20-40
Abrasives	Calcium Carbonate, Sodium Metaphosphate	20-40
Humectants	Glycerol, Sorbitol	20-40
Binders	Xanthan Gum, Carboxymethyl Cellulose	2
Surfactants	Sodium Lauryl Sulfate, Betaine	< 2
Flavors	Peppermint Oil, Eucalyptus Oil	2
Sweeteners	Saccharine, Aspartame	2
Preservatives	PHB Esters, Sodium Benzoate	<1
Colorants	Titanium Dioxide, Patent Blue V	<1
Active Ingredients	Sodium Fluoride	<1
Astringents	Zinc Citrate[3], Aluminum Lactate [4]	<2
Tartar Inhibitors	Pyrophosphate [5]	<2
Plant Extracts	Punica Granatum [6]	<2
Desensitizing Agents	Strontium Chloride [7]	1-10
Alkalizing Agents	Potassium Carbonate [8,9]	<5

Abrasives, which can constitute up to 40 % of a toothpaste's formulation, vary in size and hardness to enhance plaque removal and reduce extrinsic tooth discoloration[2,7]. By minimizing bacterial accumulation, these components support the health of both teeth and the periodontium[10]. Detergents, on the other hand, contribute to the foaming action, lowering surface tension to enhance cleaning while also acting as solubilizers for flavoring agents[7]. Fluoride, one of the most extensively studied cariostatic agents, plays a crucial role in preventing cavities by promoting natural remineralization and inhibits bacterial metabolism[11]. The caries-preventive effect primarily relies on the formation of a CaF_2-like layer of the tooth surface, serving as a fluoride reservoir that provides a sustained release of fluoride ions[12,13]. Due to its potential toxicity in high concentrations, regulatory guideline limit fluoride levels to a maximum of 1500 ppm in adult toothpastes[7]. In addition to standard toothpastes, high-fluoride formulations (e.g., 5000 ppm) are available by prescription for patients at elevated caries risk, under professional supervision[14]. Although fluoride-containing formulations remain the standard, a growing number of individuals opt for fluoride-free alternatives[15]. Beyond these core ingredients, toothpaste formulations may contain antibacterial agents, remineralizing compounds, humectants, binding agents, preservatives, and colorants, each contributing to both the clinical efficacy and the user acceptability of the product.

These substances, typically found in toothpaste formulations, can persist in the oral cavity after use and may be absorbed by oral tissues, especially if swallowed[16] (**Figure 1**). Even with thorough rinsing, certain compounds – of which not all are entirely harmless – may remain trapped in periodontal pockets, mucosal folds, or adhere to oral tissues (**Figure 1A**). From there, they may be absorbed into the systemic circulation (**Figure 1B**). This potential for systemic exposure emphasizes the importance and need for precise safety assessments of toothpaste ingredients.

To ensure consumer safety, toothpaste formulations are subject to strict regulatory guidelines, which are regularly updated to incorporate emerging scientific evidence. The EU Cosmetics Regulation provides a framework for evaluating the potential risks of various substances used in dental products[17]. Specific ingredients are either prohibited, restricted in terms of permitted concentrations and applications, or approved following toxicological evaluation. A safety report is required for each cosmetic product, and unregulated substances may only be used if the product's safety is guaranteed. The "Notes of guidance for the testing of cosmetic ingredients and their safety evaluation", prepared by the Scientific Committee on Consumer Safety (SCCS), outlines recommended protocols and criteria for toxicity testing[18].

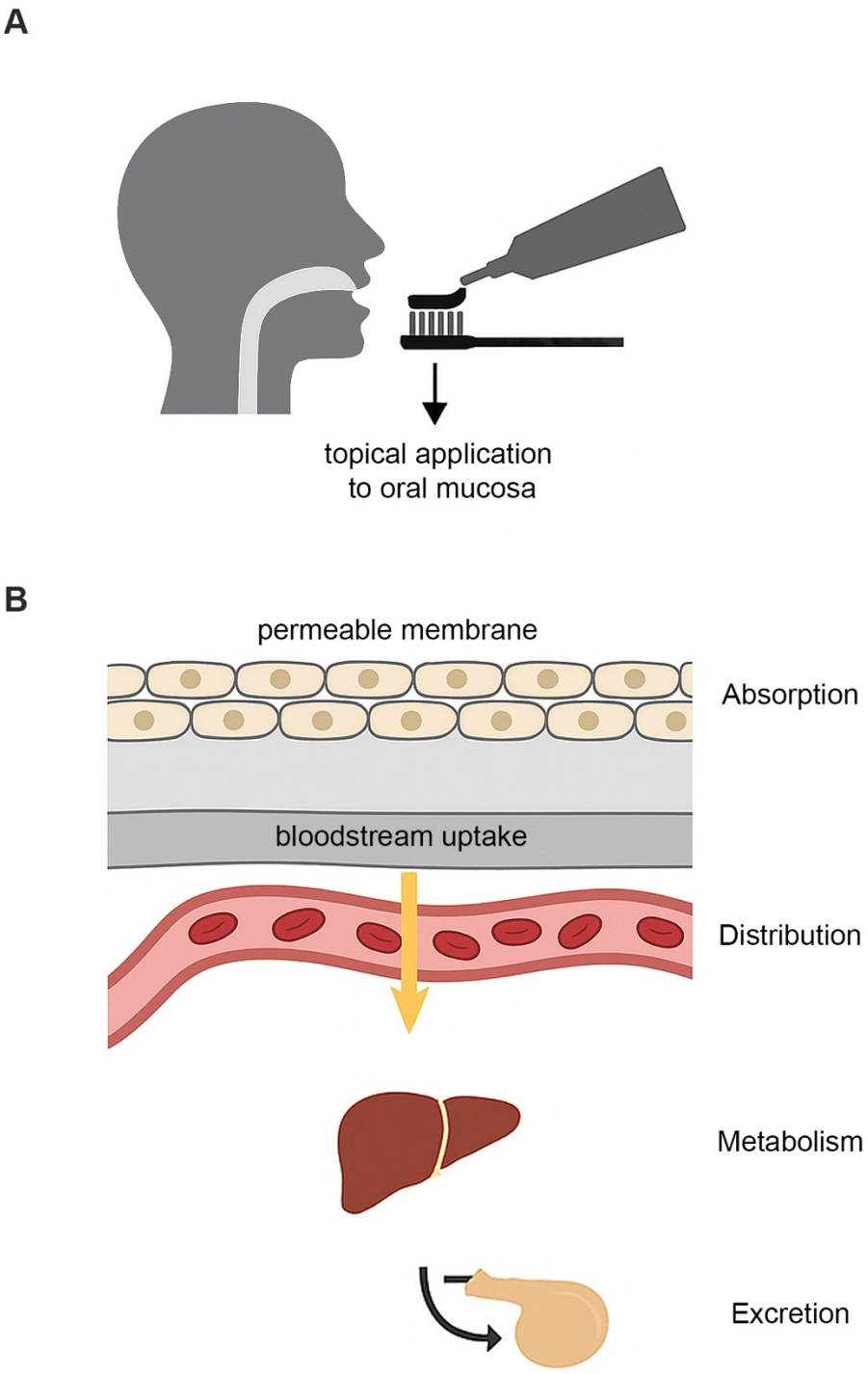

Figure 1. **Schematic representation of mucosal drug delivery: A.** Topical application of toothpaste to the oral cavity. **B.** After permeation through the epithelial layers and uptake into the capillary bloodstream, the active substance is distributed systemically, metabolized primarily in the liver, and subsequently excreted.

Recently, there has been a growing consumer trend toward natural and sustainable products, accompanied by increasing awareness of the ingredients used in both conventional and natural hygiene products (**Table 2**)**.** This shift aligns with the rise in ecological consciousness and has fueled demand for research into the safety and efficacy of natural alternatives, as well as a critical re-evaluation of synthetic formulations.

Table 2. Critical substances in toothpastes and their safety classification

Toothpaste Ingredients	Regulatory Status and Safety Assessment
Fluoride	- Permitted in toothpaste formulations up to 0,15 % (1500ppm)[19] - Considered safe at this concentration - High-fluoride formulations (e.g. 5000 ppm) are available by prescription for patients at elevated caries risk, under professional supervision [14]
Triclosan	- Allowed in cosmetics up to 0.3%[20] - banned by the US Food and Drug Administration (FDA) in hand soaps and body washes[21] - still permitted in certain toothpaste formulations based on demonstrated efficacy [21]
Titanium Dioxide	- was used in toothpaste up to 1% [22] - no longer permitted as a food additive [23] - According to the Federal Institute for Risk Assessment (BfR), no current evidence indicates harm from titanium dioxide in cosmetic products such as toothpaste[24]; however, concerns regarding genotoxicity cannot be entirely ruled out [25]
Sodium Lauryl Sulfate	- Commonly used at 0.5 – 2% in toothpaste formulations[26] - Associated with mucosal irritation and increased cytotoxicity compared to alternative surfactants [1,27] - Usage levels subject to general cosmetic safety requirements
Strontium Chloride	- Approved for use as a desensitizing agent in toothpaste (e.g., Sensodyne[28]) at 1 - 10 Vol.-%[7] - Systemic effects and potential cardiotoxicity not fully established

Potassium Carbonate	- Used in certain alternative oral care products (e.g., Pearl Shield Plus Gel Zahnpasta[29], Fango Zahncreme[30], Parodontal® Mundsalbe[31], AlkaWhite®[32], practice-based estimate is typically up to 1 - 5 % [8,9] - Not a standard ingredient in conventional toothpaste formulations, therefore limited toxicological data available, systemic and cardiotoxic effects remain poorly characterized

2.1.1. State of the Art of Strontium Chloride and Potassium Carbonate

As mentioned above, apart from conventional toothpaste, specialized formulations targeting sensitivity or whitening often incorporate additional ingredients such as strontium or potassium salts[7]. The increasing demand for desensitizing oral care products is reflected in consumer data: between 2017 and 2021, the number of individuals using sensitive toothpaste daily in Germany rose from 5.12 to 7.81 million[33]. Toothpaste formulations can vary, but Strontium Chloride ($SrCl_2$, see **Figure 2A**) is commonly used at concentrations up to 10 Vol.-% in products specifically targeting sensitivity[7] by occluding exposed dentinal tubules and forming a protective layer on the dentin surface[11,34]. Its similarity to calcium allows strontium to act in biological processes in a calcium-like way.

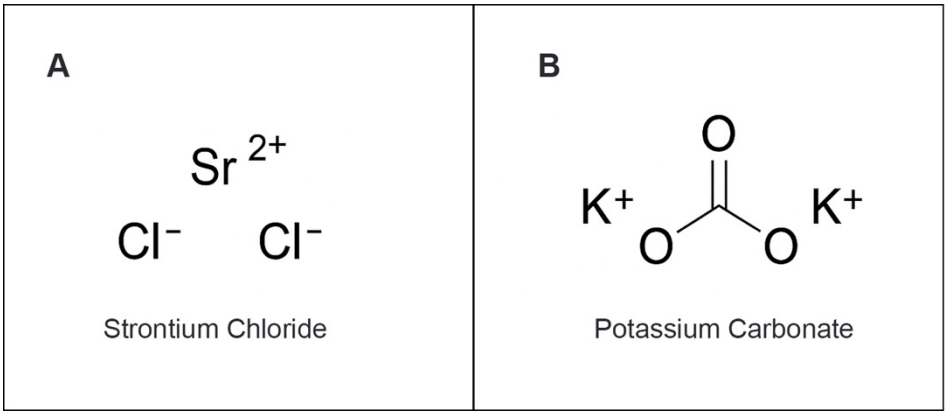

Figure 2. Chemical Structure of $SrCl_2$ and K_2CO_3. A. $SrCl_2$ consists of a divalent strontium cation (Sr^{2+}) and two chloride anions (Cl^-). In solid state, Sr^{2+} is octahedrally coordinated by six anions[35]. **B.** K_2CO_3 features a central carbonate anion (CO_3^{2-}) coordinated by two potassium cations (K^+)[35].

Several studies have demonstrated that topical application of $SrCl_2$ reduces dentin permeability and supports remineralization. *Pinto et al.*, for instance, showed that a 10% $SrCl_2$ desensitizing toothpaste significantly reduced dentinal permeability in rat teeth with partially exposed dentinal tubules[36]. Complementary to these findings, *Lippert* reported that supplementation with 1.1 mM Sr^{2+} increased enamel hardness when combined with fluoride, although without a synergistic effect on fluoridation[37]. Further supporting its clinical utility, *Alencar et al.* demonstrated that the combination of 10% $SrCl_2$ and 5% potassium nitrate reduced enamel damage during bleaching treatments[38].

Taken together, these studies highlight the potential of $SrCl_2$ as an effective agent in dental care, both for dentin hypersensitivity management and enamel protection.

Beyond dentistry, $SrCl_2$ has been applied across a broad spectrum of fields, underscoring its chemical versatility. It is used in pyrotechnics[39,40], metallurgy[41], glass ceramics[42], and atomic absorption spectroscopy[43]. In biomedical contexts, it has found applications in dermatology[44-46] and has also been incorporated into homeopathic formulations[47]. Most notably, radioactive isotopes such as $^{89}SrCl_2$ are clinically relevant in oncology, where they are used for targeted therapy of bone metastases[48]. These diverse applications illustrate the broad functional scope of $SrCl_2$ in both industrial and medical domains.

With respect to toxicological safety, available data generally indicate a favorable profile. *Akyol et al.* observed no reduction in fibroblast viability after 96 hours of exposure to concentrations up to 20%[49]. Similarly, zebrafish embryo models identified a lethal dose of approximately 6 mM, while also revealing dose-dependent effects on mineralization: low concentrations (0.0033 mM) promoted vertebral mineralization, whereas higher concentrations (0.033 – 0.33 mM) inhibited mineral deposition[50]. This biphasic response has likewise been observed in human periodontal ligament cells, where low doses of $SrCl_2$ (0.5 – 10 μg/ml) enhanced mineralization, while higher concentrations (25 – 500 μg/ml) promoted proliferation at the expense of mineral deposition[51]. Collectively, these findings suggest that $SrCl_2$ exerts concentration-dependent biological effects, which may be beneficial at lower doses but require careful consideration at higher exposures. Importantly, no evidence to date links $SrCl_2$ with carcinogenicity, genotoxicity, immunotoxicity, reproductive toxicity, neurotoxicity, or cardiotoxicity. Nevertheless, the absence of comprehensive long-term studies means that uncertainties remain, particularly regarding systemic toxicity and potential cardiac implications. Consequently, while current data support the relative safety of $SrCl_2$, further investigations is warranted to fully establish its toxicological profile in long-term and systemic contexts.

In contrast to $SrCl_2$, potassium carbonate (K_2CO_3, **Figure 2B**) in only rarely found in commercial dentifrices. As an alkalizing agent, it is primarily used to buffer pH levels in certain oral care formulations, including some natural or fluoride-free alternatives[29-31]. K_2CO_3 occurs as a hygroscopic, odorless powder that is readily soluble in water but practically insoluble in

ethanol. While potassium compounds such as potassium nitrate are well established in oral care, the efficacy of K_2CO_3 remains insufficiently characterized. Some toothpaste products containing K_2CO_3 are marketed for the treatment of dentin hypersensitivity and remineralization support. However, evidence supporting improvement in bone or tooth mineral density remains limited [52] and largely hypothetical.

Outside of oral care, K_2CO_3 is widely used in the soap and glass industries[53], chemical synthesis[54], and in homeopathy[55,56], where it is claimed to alleviate fatigue, emotional distress, and cardiovascular complaints[55]. The compound is available as a bulk chemical in pharmacies and drugstores; however, professional consultation is recommended for high-potency applications[55]. From a toxicological perspective, K_2CO_3 is classified as a caustic irritant at high concentrations. Upon ingestion or inhalation, it is absorbed via the gastrointestinal and respiratory tracts and may cause mucosal, ocular, and dermal irritation[57]. In a sub chronic toxicity study, *Akintunde et al.* exposed rabbits orally to 50 and 100 mg/L K_2CO_3 over 14 days, resulting in significant increases in serum potassium, albumin, creatine, urea, and blood urea nitrogen (BUN), suggesting hepatorenal toxicity at elevated doses[58]. Inhalation studies in rats showed reversible histological changes in nasal and lung following aerosol exposure (0.1 – 0.4 mg/L for 21 days, 6h/day), but no systemic or neurotoxic effects were detected[59]. In another *in vitro* screening for apoptosis-inducing compounds, K_2CO_3 and sodium bicarbonate at minimal concentrations induced necrotic cell death in over 78% of the mammalian cells tested[60], highlighting its potential cytotoxicity at the cellular level.

Despite its widespread use in non-dental industries, systematic safety evaluations for K_2CO_3 in oral care products are lacking. Given its possible incorporation in emerging natural formulations and its potential systemic effects, detailed toxicological investigations using advanced human-relevant in vitro models such as stem-cell derived systems are warranted.

2.2. Stem Cell Models in Drug Discovery and Toxicity Evaluation

Over the past decade, there has been a significant increase in research exploring the use of stem cells in toxicology and drug discovery. This has led to the development of new experimental models and investigational approaches, particularly involving pluripotent stem cells (PSCs) from both murine and human origin. Stem cells are undifferentiated cells defined by their self-renewal capacity and their ability to differentiate into multiple cell types[61]. They vary in origin and in the degree of differentiation, i.e., the cell potency (**Figure 3A-C**). For example, oligopotent stem cells can give rise to a limited range of cell types within a single tissue, while unipotent stem cells are restricted to a single lineage[62]. Pluripotent stem cells, such as embryonic stem cells (ESC), can differentiate into almost any cell type of the body (**Figure 3B**). In contrast, multipotent stem cells, such as adult hematopoietic stem cells, can generate several related cell types (**Figure 3C**).

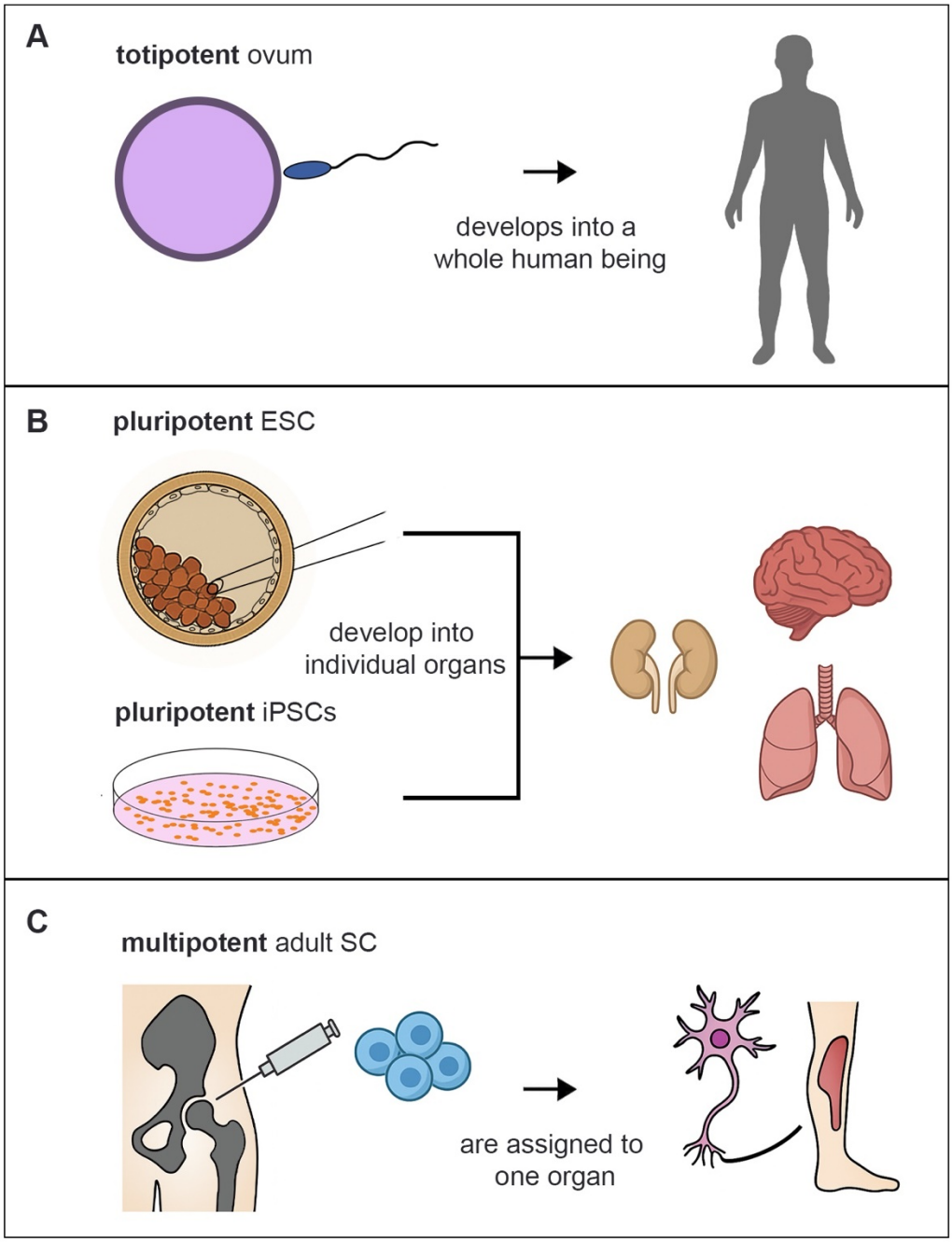

Figure 3. Developmental Potency and Origin of Stem Cells: A. Totipotent cells, such as the fertilized ovum, have the capacity to give rise to all cell types of the body and extraembryonic tissues, thereby forming a complete organism. **B.** Pluripotent stem cells, including ESC and iPSCs, can differentiate into all cell types of the three germ layers ectoderm, mesoderm, endoderm, giving rise to tissues and organs such as brain, kidney, and lungs, but not extraembryonic structures. **C.** Multipotent adult stem cells (ASCs) are tissue-resident and restricted to specific lineages within their tissue of origin (e.g. mesenchymal or hematopoietic stem cells from bone marrow). They can differentiate into specialized cell types within one organ system, such as neurons or muscle cells.

2.2.1. Embryonic Stem Cells: Applications and Limitations

ESCs are derived from early-stage embryos and can be obtained at two developmental stages: the blastomere stage and the blastocyst stage. Cells from the blastomere stage are totipotent, meaning they can give rise to all embryonic and extraembryonic tissues, and even form an entire organism (**Figure 3A**). In contrast, ESCs isolated from blastocyst, a structure that forms approximately five days after fertilization[63], are pluripotent (**Figure 3B**). These cells can differentiate into nearly all cell types of the three germ layers: ectoderm, mesoderm, and endoderm. Human embryonic stem cells (hESCs) are isolated from the inner cell mass (ICM) of the blastocyst.

Table 3. Comparison of different types of stem cells adapted from Robey [64]

	Stem Cell Types		
	ESCs	**ASCs**	**iPSCs**
Source	- Extraction from ICM of Blastocyst	- Derived from different adult tissues	- Derived from somatic cells
Scientific Advantages	- Pluripotent, can differentiate in cell types of all three germ lineages - Unlimited division	- Moderate division, can differentiate in limited cell types depending on the tissue - Autologous, no ethical issues and no teratoma risk	- Pluripotent, can differentiate in cell types of all three germ lineages - Autologous, no destruction of a blastocyst
Scientific Limitations	- Many steps required to drive differentiation into desired cell type and may be rejected - Ethical reasons because of destruction of embryo - Possibility of teratoma and allogenic	- May not be able to produce enough cells - Identification and isolation are difficult	- Possibility of teratoma - Indefinite growth
Applications	- Developmental biology studies - Potential for regenerative medicine - Disease modeling	- Tissue repair and regeneration - Potential treatments for blood disorders	- Drug testing and toxicity studies - Disease modeling and regenerative therapies

This is traditionally performed using immunosurgery, although laser-assisted isolation has been established as an alternative method[65]. Once isolated, hESCs are grown under controlled in vitro conditions. However, the use of hESCs is ethically and legally controversial due to the destruction of human embryos during isolation. These concerns have prompted the development of human induced pluripotent stem cells (hiPSCs) as a less ethically problematic alternative [66] (**Table *3***). In contrast, murine ESCs (mESCs) are commonly used in developmental and biomedical research. They can be differentiated into a wide range of cell types and are frequently employed to study the developmental potential of stem cells, as well as to investigate the effects of embryotoxic and pharmacological agents[67-69]. The efficiency of mESC culture depends on several factors, including the mouse strain and the pregnancy status of the donor female. Despite their versatility, ESCs are highly sensitive and may undergo undesired changes in culture[70-72]. To minimize the risk of tumor formation, it is crucial to establish pure lineages before further application.

2.2.2. Advances in Induced Pluripotent Stem Cell Technology

The ethical and legal challenges surrounding the use of hESCs have been the catalyst for the development of alternative, ethically less controversial sources of pluripotent stem cells (see **Figure 4**). A breakthrough method was introduced by Takahashi and Yamanaka, who demonstrated that somatic cells can be reprogrammed into a pluripotent state by ectopic expression of transcription factor such as Oct4, Sox2, Klf4 and c-Myc.

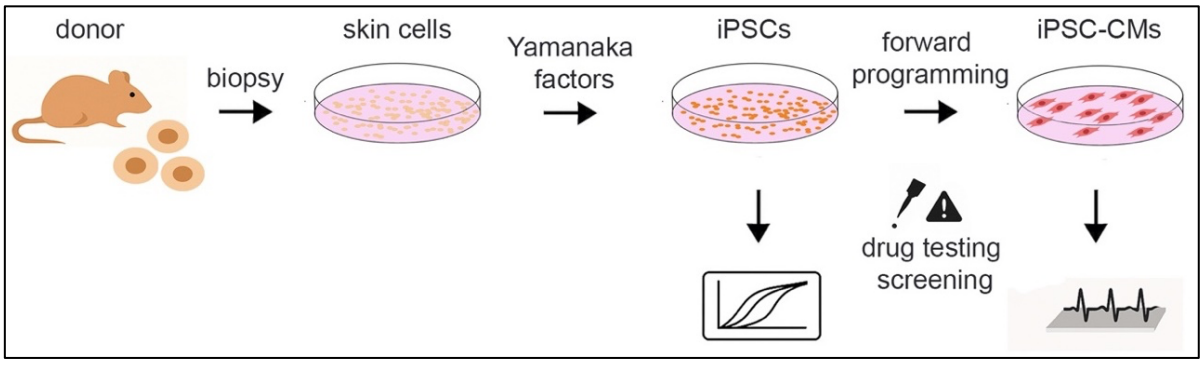

Figure 4. Reprogramming of somatic cells into iPSCs and differentiation into iPSC-CMs: Schematic overview illustrates the generation of iPSCs from somatic skin cells obtained via biopsy from a donor mouse. The somatic cells are reprogrammed into a pluripotent state using the four Yamanaka transcription factors (Oct4, Sox2, Klf4, and c-Myc). The iPSCs can subsequently be directed toward cardiac lineage through forward reprogramming to yield functional iPSC-CMs. This platform serves as a basis for cardiotoxicity screening and drug testing using electrophysiological readouts and impedance-based assays.

These iPSCs closely resemble hESCs in morphology, proliferation capacity, gene expression, and differentiation potential[73,74]. iPSCs offer a promising platform for basic research, regenerative medicine, and particularly toxicological studies due to their self-renewing capacity and pluripotency[75]. Disease-specific iPSC lines provide patient relevant models for drug testing and enhance the predictive value of compound toxicity assessments[76,77]. Various strategies have been developed to generate iPSCs and differentiate them into specific lineages. For instance, Fatima et al. employed the genetically modified murine iPSC line TiB7.4 to generate the transgenic line αPig-AT25, characterized by pluripotent colony morphology, alkaline phosphatase activity, Oct4 expression, and the surface marker SSEA1[78]. Murine iPSCs have demonstrated the capacity to differentiate into specialized cell types, including cardiomyocytes and neurons. This process is determined by differential gene activity, driven by unequal distribution of signaling molecules to daughter cells[79]. iPSC-derived cardiomyocytes (iPSC-CMs) represent a widely used *in vitro* model for evaluating cardiotoxicity. Their physiological relevance enables the detection of proarrhythmic effects of drugs, which may pose life-threatening risks to patients[80,81]. These cells also provide mechanistic insights into the pathophysiology of cardiovascular diseases. Several protocols are available for generating iPSC-CMs, including co-culture with visceral endoderm-like cells, monolayer-based 2D systems, and the widely used 3D embryoid body (EB) approach, especially in murine models[80,82-85]. EBs containing contractile areas exhibit both structural and functional characteristics of cardiomyocytes[86]. Characterization of iPSC-CMs includes analysis of cardiac transcription factors, structural proteins, ion channel expression, and Ca^{2+}-cycling machinery[87]. These properties can be accessed via techniques such as patch-clamp electrophysiology, calcium imaging, and microelectrode array (MEA) recordings. Compared to adult cardiomyocytes, iPSC-CMs exhibit immature phenotypes[88,89]. However, recent advances such as long-term culture, electrical stimulation, chemical induction, and 3D scaffolding have improved maturation[90]. Functionally and molecularly, iPSC- and ESC-derived cardiomyocytes show high similarity[91], including comparable responses to cardioactive substances[92].

2.3. Experimental Approaches for Toxicity Assessment

Stem-cell derived systems are increasingly essential in toxicological testing due to their ability to replicate human-relevant cellular responses. A variety of approaches are currently employed to assess toxicity of chemical ad cosmetic ingredients, including *in vivo*, *ex vivo*, *in vitro*, and computational (*in silico*) models. Each method has well defined advantages and limitations depending on the study objectives and biological context. *In vivo* studies, traditionally performed on animal models such as mice or rats, offers the advantages of systemic integration. The physiological similarity between species enables long-term monitoring and evaluation of complex toxic responses[93]. However, the ethical implications of animal use,

interspecies variability, and limited translational value have led to an increased focus on alternative strategies[94]. *Ex vivo* approaches involve the use of excised tissues (e.g., skin biopsies) and provide ethically preferable options with partially retained tissue architecture. These systems are suitable for studying penetration, irritation, and dermal absorption, yet they lack full systemic interaction and are prone to artefacts and short-term viability restrictions[95,96]. On the other hand, computational models use chemical structure data and established biological knowledge to predict toxicity outcome and generate hypotheses about mechanisms of action[97-102]. These methods are cost-efficient and allow for high-throughput prediction[103,104]; however, their accuracy is highly dependent on the availability and quality of curated training data and may remain unclear to non-specialists[103,105]. In contrast, *in vitro* assays allow direct testing of compounds on cultured cells under controlled laboratory conditions. These methods are widely used for cytotoxicity, genotoxicity, and irritation screening[106]. They offer high reproducibility and throughout, though they may not fully replicate the physiological complexity of a living organism[107]. Nevertheless, *in vitro* systems have become a cornerstone of modern toxicity testing, particularly due to their ethical acceptability and compatibility with stem cell-based platforms[108,109]. One such molecular-level approach is quantitative polymerase chain reaction (qPCR), which can detect transcriptional responses to toxic insult. By monitoring the expression levels of key genes involved in apoptosis, oxidative stress, or DNA repair, qPCR enables the identification of early sublethal toxic effects with high sensitivity[110]. Moreover, quantitative PCR (qPCR) allows for high sensitivity and precise quantification, enabling the early identification of sub-lethal toxic effects. Emerging technologies, such as organ-on-chip, high-throughput screening (HTS), and studies involving human volunteers, further expand the toolbox of experimental toxicology[94].

Recent advantages in stem cell-based platforms, particularly iPSC-derived cardiomyocytes, have enabled high-resolution, human-relevant toxicity testing. These systems form the basis of experimental strategies discussed in subsequent chapters of this work.

2.3.1. Cellular Analysis Approach

The evaluation of toxicity depends on a range of experimental approaches that can be categorized into cellular and functional analysis. Techniques such as immunostaining and flow cytometry provide complementary insights into cell identity, viability, and proliferation dynamics. Immunostaining is widely used to visualize the localization and abundance of specific proteins within cells or tissue sections. This method relies on antibodies directed against target proteins, which are typically combined with fluorophores or chromogens to allow detection. Immunostaining is a standard tool for validating pluripotency in iPSCs[111], confirming the differentiation status of iPSC-CMs, and verifying the purity of cardiac cultures[112,113]. While immunostaining offers spatial resolution, flow cytometry provides high-throughput, quantitative

analysis of cell populations. This technique is particularly useful for distinguishing between viable and non-viable cells in response to toxic insults. One commonly used marker is propidium iodide (PI), a membrane-impermeable dye that selectively stains the DNA of dead or dying cells with compromised membrane integrity[114,115]. In contrast, viable cells exclude PI, resulting in low background fluorescence. This enables a precise quantification of drug-induced cytotoxicity within defined cell populations. Another approach frequently used in toxicity studies is the mentioned qPCR. This method allows for the sensitive detection and quantification of transcriptional changes, such as the expression of genes related to apoptosis, DNA repair, or stress response. By analyzing these early molecular responses, qPCR provides valuable mechanistic insights, that complement protein-level and functional readouts[110]. Together, these approaches provide both qualitative and quantitative metrics of toxicity induced changes at the cellular level.

2.3.2. Functional Assessment Techniques

To complement morphological and viability analyses, functional assessment tools such as the xCELLigence Real-Time Cell Analysis (RTCA) system (**Figure 5A-C**) and Multi-Electrode Array (MEA) technology have become integral in toxicity testing. These systems allow for continuous, label-free monitoring of dynamic biological processes such as cell growth, morphological changes, and electrical activity, particularly in cardiomyocytes[116-122].

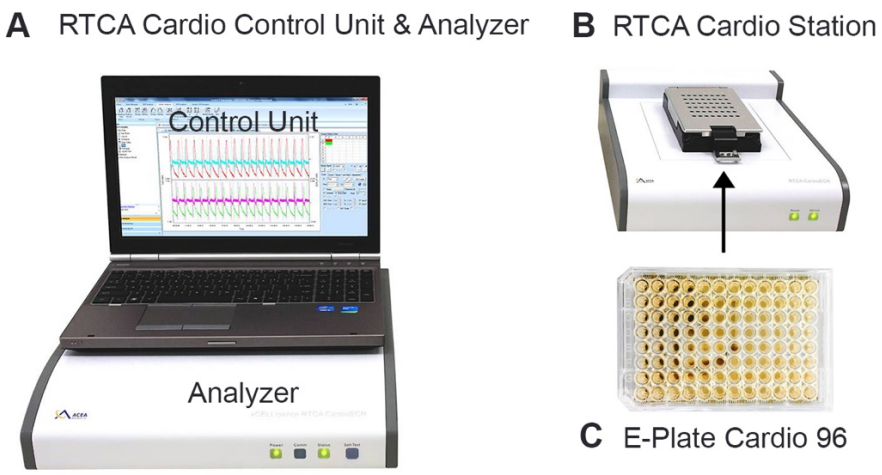

Figure 5. The xCELLigence RTCA Cardio Instrument: This System consists of four main components: **A.** the RTCA Cardio Control Unit and Analyzer, **B.** the RTCA Cardio Station, and **C.** the 96-well electronic microtiter plate (E-Plate Cardio 96) (adapted from Accela)[123]. The arrow indicates the insertion of **C.** the E-Plate Cardio 96 into **B.** the RTCA Cardio Station for measurement.

The xCELLigence RTCA system utilizes impedance-based measurements to monitor cell adhesion, proliferation, and cytotoxicity in real time. This method has been successfully applied across various fields, including environmental toxicology, microbiology, and cardiac research[124-128]. In the context of stem cell-based studies, RTCA has proven valuable for evaluating compound-induced effects on iPSC-CMs, capturing both acute and long-term responses[128]. In parallel, MEA recordings enable extracellular measurement of field potentials, providing functional readouts of electrical activity in cardiomyocytes[129,130]. This technique is particularly suited for detecting arrhythmic events, conduction abnormalities, and drug-induced alterations in electrophysiological behavior[131,132]. The combination of MEA and RTCA technologies enables a multi-dimensional analysis of compound effects, capturing both electrophysiological and morphodynamical parameters in real time.

2.4. Aim of Study

Currently, screening for potential toxicity of chemical ingredients is an important part of medical research. Despite their use in toothpastes, the potential cardiotoxic effects of $SrCl_2$ and K_2CO_3 remain insufficiently characterized. Previous studies have not demonstrated carcinogenic or neurotoxic properties of these compounds; however, systematic assessments of their impact on cardiac function and stem cell behavior are lacking.

The primary objective of this study was threefold:

(i) to investigate the proliferative effects of $SrCl_2$ and K_2CO_3 across various concentrations on undifferentiated iPSCs.

(ii) to determine the arrhythmogenic potential of these compounds using iPSC-CMs under controlled *in vitro* experimental setting, focusing on their ability to induce toxic responses or arrhythmias over prolonged exposure.

(iii) to examine gene expression changes related to stress response and apoptosis in iPSC-CMs after compound exposure using quantitative PCR.

To achieve this, a multimodal analysis strategy was employed combining real-time impedance monitoring (xCELLigence RTCA), qRT-PCR, FACS, and MEA recordings. These complementary approaches enable a more comprehensive understanding of the toxicological profile of $SrCl_2$ and K_2CO_3, with relevance to their implications for cardiac health and their potential therapeutic applications.

3. Materials and Methods

3.1. Chemicals, Media, and Drugs

All cell culture media and supplements were purchased from Thermo Fisher Scientific (Germany); unless otherwise noted. Chemicals and test compounds were purchased from Carl Roth (Germany) or Sigma-Aldrich (Germany). A comprehensive list of reagents, including final working concentrations and suppliers, is provided in **Table 4**.

Table 4. Cell culture media, supplements, and drugs

Substances	Final Concentration	Supplier
Cell Culture Reagents		
DMEM+GlutaMAX	83 %	Thermo Fisher Scientific GmbH
FBS	1% (FACS) 15 % (AT25-culture)	Thermo Fisher Scientific GmbH
MEM-NEA	1 X	Thermo Fisher Scientific GmbH
Penicillin-Streptomycin	1 X	Thermo Fisher Scientific GmbH
ß-Mercaptoethanol	50 µM	Thermo Fisher Scientific GmbH
LIF	1 U/ml	Thermo Fisher Scientific GmbH
G418 (Neomycin)	0,5 mg/ml	Thermo Fisher Scientific GmbH
PBS	1 X	Thermo Fisher Scientific GmbH
Trypsin/EDTA	0.05 %	Thermo Fisher Scientific GmbH
Staining & Analysis		
PI	10 µg/ml	Thermo Fisher Scientific GmbH
Hoechst 33342	1 µg/ml	Thermo Fisher Scientific GmbH
α-Actinin Antibody	1:500	Sigma-Aldrich
Triton X-100	0.25%	Sigma-Aldrich
Ammonium Chloride	0.5 M	Sigma-Aldrich
BSA	0.8%	Sigma-Aldrich
Matrigel	undiluted	Corning (USA)
Gelatin	0.1%	Sigma-Aldrich
Puromycin	8 µg/ml	Thermo Fisher Scientific GmbH
IMDM + GlutaMAX		Thermo Fisher Scientific GmbH
Trypan Blue	0.4 %	Thermo Fisher Scientific GmbH
Test Compounds		
$SrCl_2$	0.07 to 3.15 mM	Carl Roth
K_2CO_3	0.1 to 3.2 mM	Carl Roth

3.2. Cells Culture and Differentiation Protocols

3.2.1. Maintenance of Undifferentiated iPSCs

The murine iPSC line AT25 was maintained on neomycin-resistant feeder layers in DMEM supplemented with 15% FBS, 1X NEAA, 2X Pen/Strep, 50 µM ß-Mercaptoethanol, and 1 U/mL leukemia inhibitory factor (LIF). Cells were passaged every two days using 0.05% trypsin/EDTA. After detachment at 37°C for 3-5 minutes, cells were neutralized with medium, centrifuged, resuspended in fresh culture medium, and seeded onto new plates. Cell viability and density were determined using trypan blue exclusion. Dissociated cells were either used for subsequent passaging or downstream applications (e.g., FACS, MEA).

3.2.2. Differentiation of iPSCs into Cardiomyocytes

Cardiac differentiation was performed as previously described[133]. Briefly, undifferentiated iPSCs were transferred to non-adherent conditions and cultured in IMDM + GlutaMAX medium supplemented with 20% FBS, 0.1 mM NEAA, 0.1 mM ß-mercaptoethanol, and 50 µg/mL Pen/Strep to induce EB formation. Contractile EBs typically appeared after 7-10 days. eGFP expression was used to confirm cardiomyocyte identity prior to puromycin selection. The purity of selected populations was confirmed microscopically based on fluorescence intensity. Surviving clusters were dissociated into single cardiomyocytes, pre-plated for 24 hours, and subsequently seeded onto MEA chips or E-Plates for downstream functional assays (xCELLigence RTCA, MEA).

3.3. Experimental Models and Tools

3.3.1. Immunostaining

Immunocytochemistry was performed to assess the differentiation status of iPSC-CMs via detection of sarcomeric α-actinin and nuclear morphology. Following dissociation, iPSC-CMs were replated on Matrigel-coated plates and cultured for two days. Cells were fixed with 4% paraformaldehyde (PFA) for 20 minutes at room temperature (RT) and subsequently washed three times with Dulbecco's phosphate-buffered saline (DPBS). Permeabilization was achieved using 0.25% Triton X-100 in Trish wash buffer for 10 minutes. To block non-specific binding, Roti-Immune Block (Carl Roth, Germany) was applied for 1 hour at RT. Cells were then incubated with the primary antibody mouse anti-α-actinin (1:500, Sigma-Aldrich) for 2 hours at RT. After washing three times, fluorescent secondary antibodies were applied for 1 hours. Nuclei were counterstained with Hoechst 33342 (1 µg/ml, Thermo Fisher) for 10 minutes. Samples were imaged using an Apotome fluorescence microscope.

3.3.2. FACS Analysis of iPSCs

To quantify the viability of undifferentiated iPSCs following compound exposure, FACS analysis was performed using PI exclusion. Cells were treated with $SrCl_2$ (0.16 mM and 3.15 mM) and K_2CO_3 (0.2 mM and 3.2 mM) for 24 and 72 hours. Compounds and medium were refreshed daily. After treatment, cells were washed with PBS and dissociated with 0.05 % Trypsin-EDTA at 37°C for 2-3 minutes. Trypsin activity was neutralized by DMEM supplemented with 20% FBS. After centrifugation (5 minutes, 1000 rpm), the pellet was resuspended in PBS, filtered through a 40 μm strainer, and stained with 10 μg/ml PI for 10-15 minutes at RT. Data acquisition was performed on a FACSAria II flow cytometer, and results were analyzed using FlowJo v7 software.

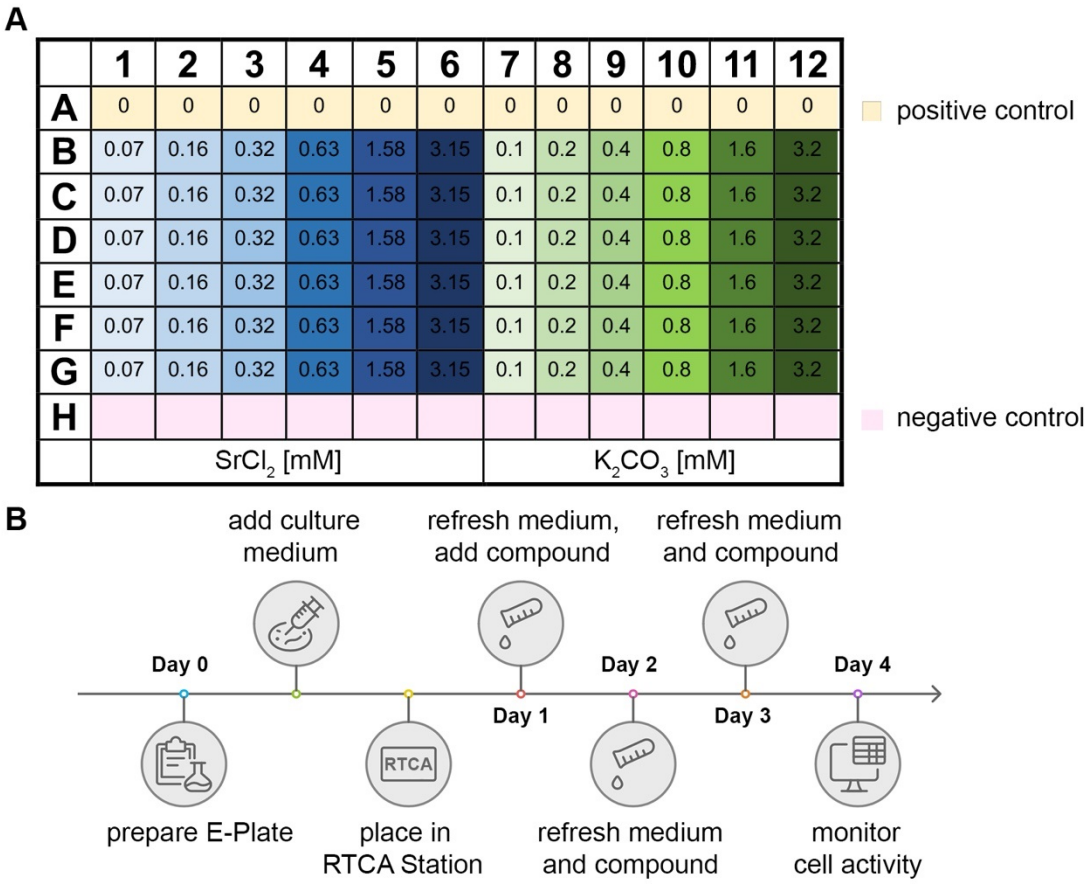

Figure 6. Schematic overview of the experimental workflow for real-time proliferation monitoring of iPSCs using the xCELLigence RTCA Cardio Instrument: A. Different concentrations of the compound were used for this study and distributed on the E-Plate Cardio 96. **B.** Preparation of the E-Plate took place on the same day as plating the iPSCs. The medium and the compound were renewed every 24 hours, until data analysis occurred.

3.3.3. Field Proliferation and Electrical Activity Monitoring via xCELLigence

Real-time analysis of cell viability and cardiomyocyte function was performed using the xCELLigence RTCA system. E-Plate Cardio 96 wells were precoated with 0.1% gelatin and incubated for 30 minutes at 37°C to create a supportive surface and enhance cell attachment (**Figure 6 A-B**). After aspirating gelatin, fresh culture medium was added, and background impedance measured. iPSCs and iPSC-CMs were seeded and treated with increasing concentrations of $SrCl_2$ (0.07 - 3.15 mM) and K_2CO_3 (0.1 - 3.2 mM). Culture medium and compounds were refreshed every 24 hours over a 72-hour period. Cell index (CI) and beating profiles (amplitude and frequency) were recorded continuously. Data were analyzed using the RTCA Cardio software.

3.3.4. Potential Measurements Using MEA

The electrophysiological activity of iPSC-CMs was measured using a MEA system. MEA chips were coated with 0.1 % gelatin and incubated for 1 hour at 37°C. After removing the coating solution, $1x10^6$ purified iPSC-CMs were seeded per well and cultured in differentiation medium (500µl/well) for 48 hours. Baseline measurements were acquired prior to compound application. Subsequently, cells were exposed to varying concentrations of $SrCl_2$ and K_2CO_3. For each concentration, field potentials were recorded for 3 minutes. Experiments were independently replicated ($SrCl_2$ n=3, K_2CO_3 n=4). Data including corrected field potential duration (FPDc), amplitude, and beating frequency were analyzed using McRack software.

3.3.5. Gene Expression Analysis by qRT-PCR

To evaluate gene expression changes in iPSC-CMs after compound exposure, qRT-PCR was performed. Total RNA was isolated from untreated and treated cells using TRIzol reagent according to the manufacturer's protocol (**Table 5**). RNA quality and concentration were assessed via NanoDrop. Samples with A260/A280 ratios between 1.8 and 2.0 were used for reverse transcription. Complementary DNA (cDNA) was synthesized from 1µg RNA using random hexamers, dNTPs, RNAse inhibitor, DTT, and Reverse Transcriptase. Reactions were carried out at 37 °C for 15 minutes, 72 °C for 10 minutes, and 42 °C for 50 minutes. qRT-PCR was performed using SXBR Green SuperMix on a 7500 Fast Real-Time PCR System. Target genes included cardiac-specific markers (e.g., *Myl2, Myh6, Nppa*), ion channel genes *(*e.g., *Scn5a, Cacna1c, Kcnh2*), and transcription factor (e.g., *Mesp1*), normalized to *Gapdh*. Primer sequences are listed in **Table 6**. The ΔΔCt method was used for relative quantification, and data were expressed as fold changes relative to untreated control.

Table 5. Reagents and enzymes used for RNA extraction, cDNA synthesis, and qRT-PCR

Substances	Purchased from
TRIzol Reagent	Gibco BRL
Chloroform	AppliChem GmbH
Isopropanol	AppliChem GmbH
DEPC-treated water	Thermo Fisher Scientific GmbH
Random Primer	Thermo Fisher Scientific GmbH
dNTP Mix (10 mM)	Thermo Fisher Scientific GmbH
RNAse Inhibitor	Thermo Fisher Scientific GmbH
First Strand Buffer	Thermo Fisher Scientific GmbH
DTT	Thermo Fisher Scientific GmbH
Reverse Transcriptase	Thermo Fisher Scientific GmbH
JumpStart Taq Mix	Sigma-Aldrich
SYBR Green qPCR SuperMix	Thermo Fisher Scientific GmbH
cDNA Synthesis Kit	Life Technologies
Gene-specific Primers (GAPDH, CACNA1C, etc.)	Sigma-Aldrich

Table 6. Mouse Primer List

Gene	Forward Primer (5'→3')	Reverse Primer (5'→3')
Gapdh	GGTGCTGAGTATGTCGTGGA	CGGAGATGATGACCCTTTTG
Cacna1c	AAGGCTACCTGGATTGGATCAC	GCCACGTTTTCGGTGTTGAC
Scn5a	GAAGAAGCTGGGCTCCAAGA	CATCGAAGGCCTGCTTGGTC
Kcnh2	CGTGCTGCCTGAGTACAAGCT	TGTGAAGACAGCCGTGTAGATGA
Myh6	AACAGGTGATGGCAAGATCC	GCTCAAAGTCAGCACCTTC
Mlc2V	AAAGAGGCTCCAGGTCCAAT	TCAGCCTTCAGTGACCCTTT
Mesp1	GTCTGCAGCGGGGTGTCGTG	CGGCGGCGTCCAGGTTTCTA
Nppa	GGGGGTAGGATTGACAGGAT	ACACACCACAAGGGCTTAGG
Myl2	AAAGAGGCTCCAGGTCCAAT	TCAGCCTTCAGTGACCCTTT

3.4. Data Acquisition and Statistical Analysis

Raw data were either analyzed using the respective manufacturer-provided software tools (xCELLigence RTCA software, McRack, FlowJo v7), or exported as Excel or .txt formats for further processing. For each independent experiment, results were normalized to the corresponding untreated control group, defined as 100% at each time point. The normalized values were calculated by dividing the measured values of each treatment condition by the mean control value of the respective experiment and time point. Statistical analyses were performed using SigmaPlot. Differences between groups were assessed using unpaired two-tailed Student's t-test. A p-value of <0.05 was considered as statistically significant, while p-values of >0.05 were regarded as non-significant. Data were visually rounded to two decimal places for improved readability; however, all statistical calculations were based on the original, unrounded values to preserve analytical accuracy.

4. Results

4.1. Culture of iPSCs and differentiation of iPSC-CMs

The murine iPSC line AT25 was successfully maintained under standard culture conditions on a neomycin-resistant feeder layer. Cells exhibited characteristic compact colony morphology with clear cell boundaries and homogenous distribution, consistent with the undifferentiated pluripotent state (**Figure 7A-B**). The cells proliferated robustly and retained their typical morphology over multiple passages. Cardiac differentiation was initiated via EB formation. Within 7-9 days, spontaneously contracting EBs developed, with eGFP-positive regions indicating transgene activation under the α-myosin heavy chain promoter (α-MHC), marking the onset of cardiomyocyte lineage commitment (**Figure 7C**). Fluorescence intensity and pattern corresponded to functional differentiation zones. To confirm successful differentiation at the cellular level, immunofluorescence staining was performed after EB dissociation. Surviving adherent cells were stained for α-actinin, a sarcomeric marker of cardiomyocytes (**Figure 7D**), and nuclei were counterstained with DAPI (**Figure 7E**). Overlay of both channels confirmed cytoskeletal organization and nuclear density in differentiated cardiomyocyte-like cells (**Figure 7F**) consistent with successful structural maturation.

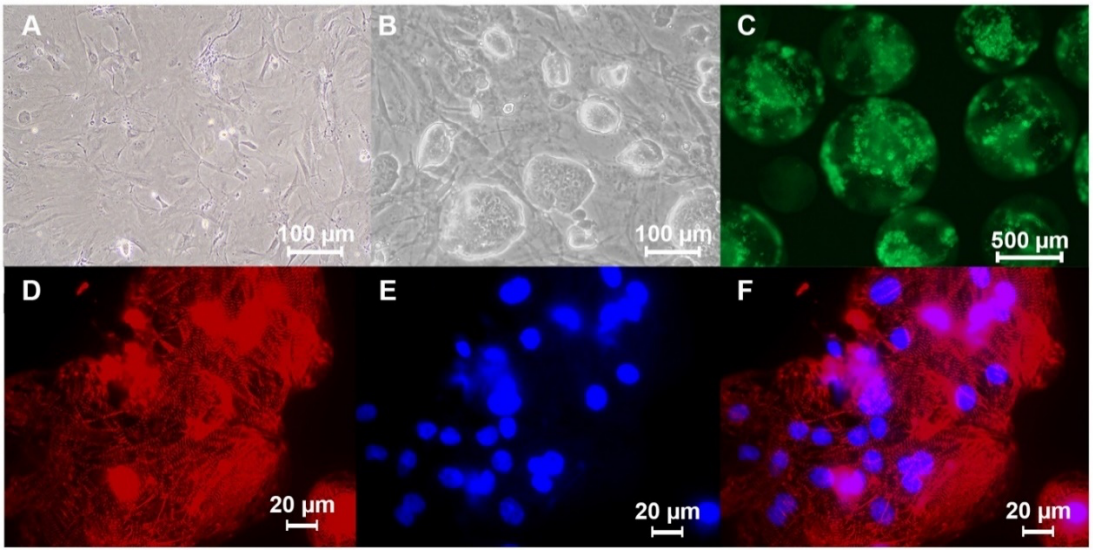

Figure 7. Representative images of murine iPSCs and 3D differentiated cells: **A-B.** Undifferentiated murine iSPCs cultured on neomycin-resistant feeder layers forming compact colonies. **C.** Spontaneously beating EBs, expressing eGFP under control of the α-MHC promoter. **D.** Immunofluorescence staining for α--actinin (red). **E.** Nuclear counterstain with DAPI (blue). **F.** Merged channels showing sarcomeric organization and cellular density.

4.2. Impact of $SrCl_2$ and K_2CO_3 on iPSCs Proliferation

To evaluate the effects of $SrCl_2$ and K_2CO_3 on iPSCs proliferation and viability, impedance-based real-time monitoring was performed using the xCELLigence RTCA system over a 72-hour period. The CI values were normalized to the respective untreated control at each time point, and FACS analysis of dead cells was additionally conducted to validate cytotoxicity.

Across the three independent experiments, $SrCl_2$ exposure consistently influenced cell proliferation in a concentration- and time dependent manner, though the specific response profiles varied slightly between replicates. In the first experiment (**Table 7A**), a consistent decline of CI values was observable at higher $SrCl_2$ concentrations, significantly at 3.15 mM after 72 h (51.93%, $p<0.05$), indicating cytotoxicity following prolonged exposure.

Table 7. Percentage change in CI values of iPSCs relative to control after 72-hour $SrCl_2$ treatment (*p<0.05 vs. control at respective time point).

A. Experiment 1

Time	0.07 mM	0.16 mM	0.32 mM	0.63 mM	1.58 mM	3.15 mM
0h	68,36	120,11	95,19	114,28	124,01	68,46
6h	67,21	118,95	97,26	135,42	158,16	113,76
12h	65,25	119,27	119,91	123,2	141,04	97,59
24h	61,93	101,63	85,95	104,23	109,79	78,9
48h	58,33	87,2	81,9	97,5	86,24	59,22
72h	58.17	80,51	78,36	89,9	75,52	51,93*

B. Experiment 2

Time	0.07 mM	0.16 mM	0.32 mM	0.63 mM	1.58 mM	3.15 mM
0h	129,21	104,12	135,7	134,51	124,98	143,91
6h	98,46	91,5	133,82	143,01*	129,54*	186,4*
12h	90,98	101,1	108,16	113,35	90,12*	152,73*
24h	67,74	63,37	73,85	57,91	43,81	59,38*
48h	73,83	83,93	77,26	42,42	34,43	43,75*
72h	75,34	83,45	76,35	38,53	32,9	46,17*

C. Experiment 3

Time	0.07 mM	0.16 mM	0.32 mM	0.63 mM	1.58 mM	3.15 mM
0h	106,14	124,98	110,76	177,49	185,27	67,9
6h	150,03	257,08*	190,04	299,69	165,28	182,49
12h	134,14	207,35*	130,73	241,91	120,83	142,72
24h	132,23	185,08*	181,97*	178,47	185,64	98,19
48h	157,53	213,57*	266,16*	222,48*	202,65	105,99
72h	156,48	179,4*	206,61*	171,68*	132,61	121,95

Intermediate concentrations (0.32 – 1.58 mM) induced transient increases in CI within the first 6-12 hours, followed by consistent decreases thereafter. A different biphasic response appeared in the second dataset (**Table 7B**), where moderate doses induced a short-term stimulatory effect within the first 6 h (up to 186.4%, $p<0.05$), followed by a progressive decline until 72 h (3.15 mM with 46.17%, $p<0.05$). Contrastingly, the third experiment (**Table 7C**) showed a robust proliferative response across multiple concentrations, with peak effects at 48 h and 72 h and without measurable cytotoxicity, highlighting strong interexperimental variability. **Figure 8A-a** summarizes the mean CI changes for all experiments (n=3). While low to moderate concentrations initially promoted proliferation, higher concentrations resulted in reduced CI values over time. Specifically, 0.16 mM $SrCl_2$ significantly increased proliferation at early time points (6-24 h), while prolonged exposure showed no further benefit (**Figure 8A-b**). In contrast, 3.15 mM led to a significant suppression of proliferation from 24 h to 72 h treatment compared to control (**Figure 8A-c**). Complementary FACS analysis confirmed increased cell death with higher $SrCl_2$ concentrations (**Figure 8A-d, e**). At 24 h, PI-positive cells increased slightly, intensifying at 72 h with 8.36% at 0.16 mM and 11.98% at 3.15 mM ($p<0.05$), validating the CI-based results in Experiment 1 - 2 and confirming a concentration- and time-dependent cytotoxic effect of $SrCl_2$ at high doses.

The effects of K_2CO_3 on iPSC proliferation followed a similar pattern of concentration dependence. In the first dataset (**Table 8A**), CI initially ranged between 111.16% and 145.04% of control at 0h, followed by a progressive decline across all concentrations. At the highest concentration (3.2 mM), a significant reduction in CI was already observed at 48 h (45.71%, $p<0.05$) and became more pronounced by 72 h (31.28%, $p<0.05$), indicating clear cytotoxicity upon prolonged exposure. Similar dynamics were observed in the second replicate (**Table 8B**), where decreases at 1.6 mM and 3.2 mM starting from 24 h onward (32.73% and 41.83%, respectively; $p<0.05$) and persisted through 72 h (41.99% and 58.57%, $p<0.05$), suggesting consistent cytotoxicity at higher concentrations. In contrast, the third experiment (**Table 8C**) showed a faster and broader decline across all concentrations. Although some recovery at lower doses was observed by 72 h, the CI at 3.2 mM still showed a significant reduction (44.03%; $p<0.05$). A comparison of the three technical replicates reveals a consistent, reproducible dose- and time-dependent cytotoxic effect of K_2CO_3. The shared decrease in CI is summarized in **Figure 8B-f-h**, emphasizing the consistency of the cytotoxic response.

To further validate the viability data, FACS after 24 h showed a slightly higher proportion of PI-positive (dead) cells, further increasing until 10.35 % at 0.2 mM and 16.16% at 3.2 mM after 72 h ($p<0.05$, **Figure 8 B-j**), supporting a concentration- and time dependent cytotoxic effect in K_2CO_3 treated iPSCs.

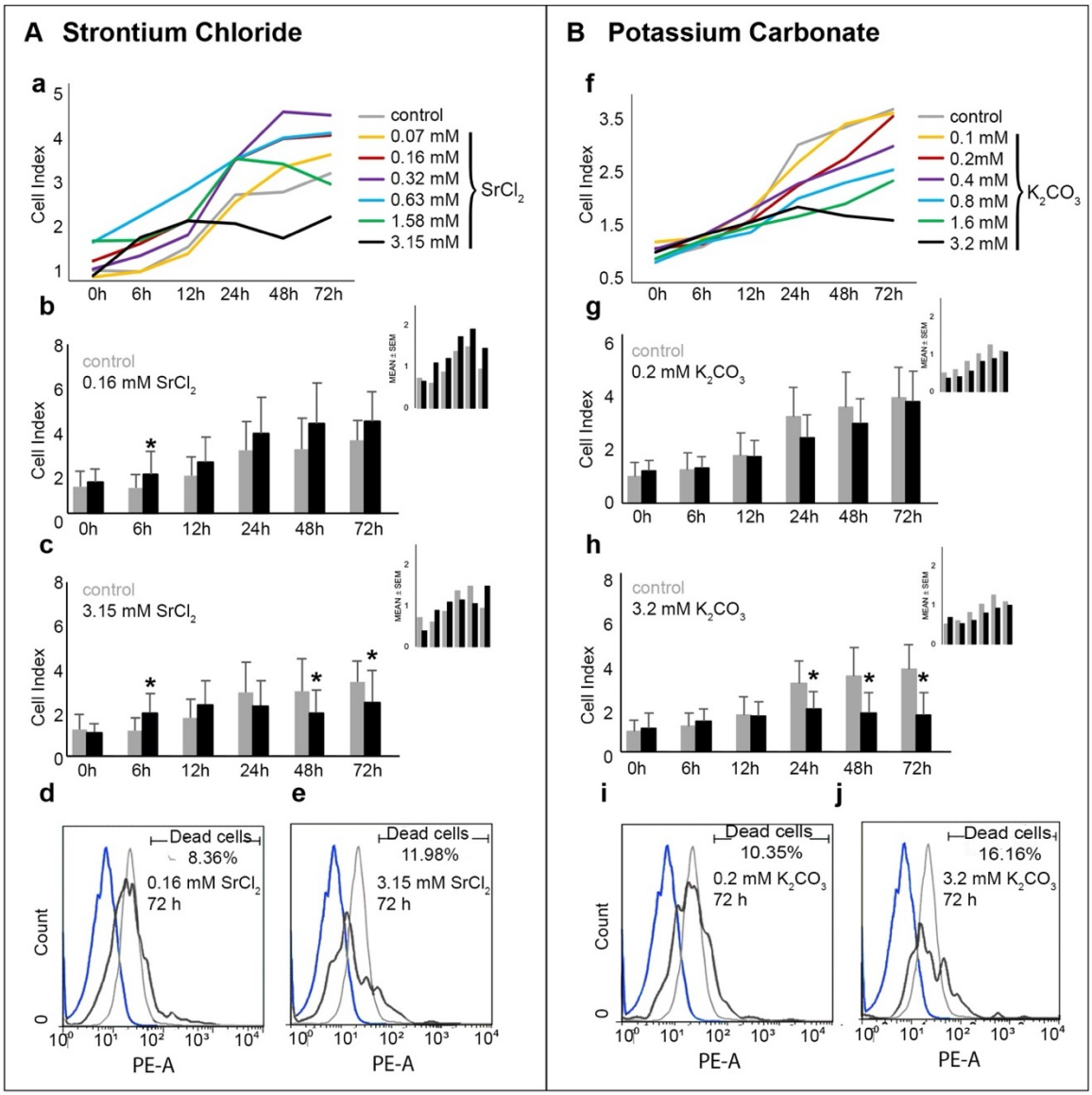

Figure 8. Effects of $SrCl_2$ and K_2CO_3 on iPSCs Proliferation and Viability: A. Overview of real-time proliferation and cytotoxicity profiles for murine iPSCs treated with increasing concentrations of $SrCl_2$. **a.** Real-time proliferation curves (mean CI, n=3) across all concentrations (0.07 – 3.15 mM) over 72 h. **b.** Bar graphs showing CI changes after treatment with 0.16 mM and **c.** 3.15 mM $SrCl_2$, demonstrating an inhibitory effect over time. **d-e.** Representative histograms from FACS analysis after 72 h PI staining at **d.** 0.16 mM and **e.** 3.15 mM $SrCl_2$, showing elevated proportions of non-viable cells compared to control. **B.** Analysis of proliferation and cytotoxic effects of K_2CO_3 on iPSCs. **f.** real-time proliferation curves, **g.** bar graphs showing CI progression with 0.2 mM and **h.** 3.2 mM K_2CO_3 across 72h. **I-j.** FACS results after 72h PI staining for **i.** 0.2 mM and **j.** 3.2 mM K_2CO_3, showing dose-dependent cytotoxicity. Data are expressed as mean ± SEM (n=3-4).

Table 8. Percentage change in CI values of iPSCs relative to control after 72-hour K_2CO_3 treatment (*p<0.05 vs. control at respective time point).

A. Experiment 1

Time	0.1 mM	0.2 mM	0.4 mM	0.8 mM	1.6 mM	3.2 mM
0h	139,52	111,16	137,01	122,94	112,52	145,04
6h	126,07	99,2	141,56	128,03	137,16	131,74
12h	150,2	116,17	146,51	128,49	134,97	123,22
24h	115,61	92,99	106,13	91,75	95,83	89,2
48h	92,54	81,39	86,46	83,1	71,87	45,71*
72h	86,5	80,68	84,44	77,82	70,21	31,28*

B. Experiment 2

Time	0.1 mM	0.2 mM	0.4 mM	0.8 mM	1.6 mM	3.2 mM
0h	133,13	140,75	127,7	108,65	84,3	65,98
6h	126,59	131,66	145,09	124,11	107,62	110,54
12h	100,63	104,8	121,59	103,78	75,26	78,27
24h	78,59	74,06	78,04	67,2	32,73*	41,83*
48h	90,28	68,32	74,14	65,51	29,94*	28,64*
72h	98,21	106,73	86,78	74,14	41,99*	58,57*

C. Experiment 3

Time	0.1 mM	0.2 mM	0.4 mM	0.8 mM	1.6 mM	3.2 mM
0h	100,31	117,36	66,01	42,4	92,42	101,03
6h	66,09	91,97	50,93	76,88	85,11	112,38
12h	62,53	76,57	41,99	36,99	66,82	87,73
24h	54,37	59,11	29,48	43,6	47,4	60,43
48h	108,35	103,31	47,77	39	84,35	114,05
72h	116,32	102,08	51,36	50,3	89,37	44,03*

A comparison between the effects of $SrCl_2$ and K_2CO_3 on iPSC proliferation reveals distinct toxicity profiles. K_2CO_3 showed a more uniform and reproducible decline in CI across all three replicates, particularly at 3.2 mM, where the CI dropped below 50% after 48 – 72h. $SrCl_2$, in contrast, produced more heterogeneous responses, combining proliferative effects at intermediate concentrations with cytotoxicity in two out of three experiments at the highest dose. In summary, both compounds induced cytotoxic effects at high concentrations (3.15 mM $SrCl_2$, 3.2 mM K_2CO_3), but the reproducibility and pattern of toxicity differ significantly with K_2CO_3 exerting a steadier and more predictable toxicity profile.

4.3. Cardiotoxic Effects of $SrCl_2$ and K_2CO_3 on iPSC-CMs

To evaluate the cardiotoxic effects of $SrCl_2$ and K_2CO_3, murine iPSCs (AT25 line) were differentiated into beating cardiomyocytes (iPSC-CMs). As shown in **Figure 9A**, both $SrCl_2$ and K_2CO_3 resulted in an initial increase in CI values across all tested concentrations, indicating successful cell attachment and early maturation. However, prolonged exposure to 3.2 mM of either compound led to a gradual decline in CI after 72 h, with K_2CO_3 causing a more pronounced reduction compared to $SrCl_2$. Lower concentrations (0.6 mM and 1.6 mM) maintained stable CI values over time, comparable to untreated controls, suggesting no overt cytotoxicity at these doses. Contractile behavior was analyzed using the beating profile traces recorded by the RTCA system (see **Figure 9B**). For $SrCl_2$, regular and rhythmic contraction patterns were observed at 0.6 and 1.6 mM. At 3.2 mM, contractions remained rhythmically organized but exhibited decreased amplitude and frequency. In contrast, 3.2 mM K_2CO_3 treatment induced more severe impairments, causing irregular, low-amplitude contraction profiles, suggestive of disrupted excitation-contraction coupling and early signs of functional failure. Quantitative analysis of beating frequency (**Figure 9C**) confirmed these observations. For $SrCl_2$, a significant decrease in beating rate was only observed at the highest concentration (3.2 mM; $p<0.05$). K_2CO_3, however, caused a concentration-dependent reduction in beating rate starting from 1.6 mM, with a pronounced drop below 100 bpm at 3.2 mM ($p<0.05$), indicating a stronger and earlier functional impairment. Taken together, these findings reveal that both $SrCl_2$ and K_2CO_3 negatively impact iPSC-CM contractility in a dose-and time-dependent manner. However, K_2CO_3 exhibits a more substantial and earlier decline in function, evident in both CI progression and contraction frequency. This underscores the importance of compound-specific toxicity profiling using real-time functional assays in iPSC-derived cardiac models.

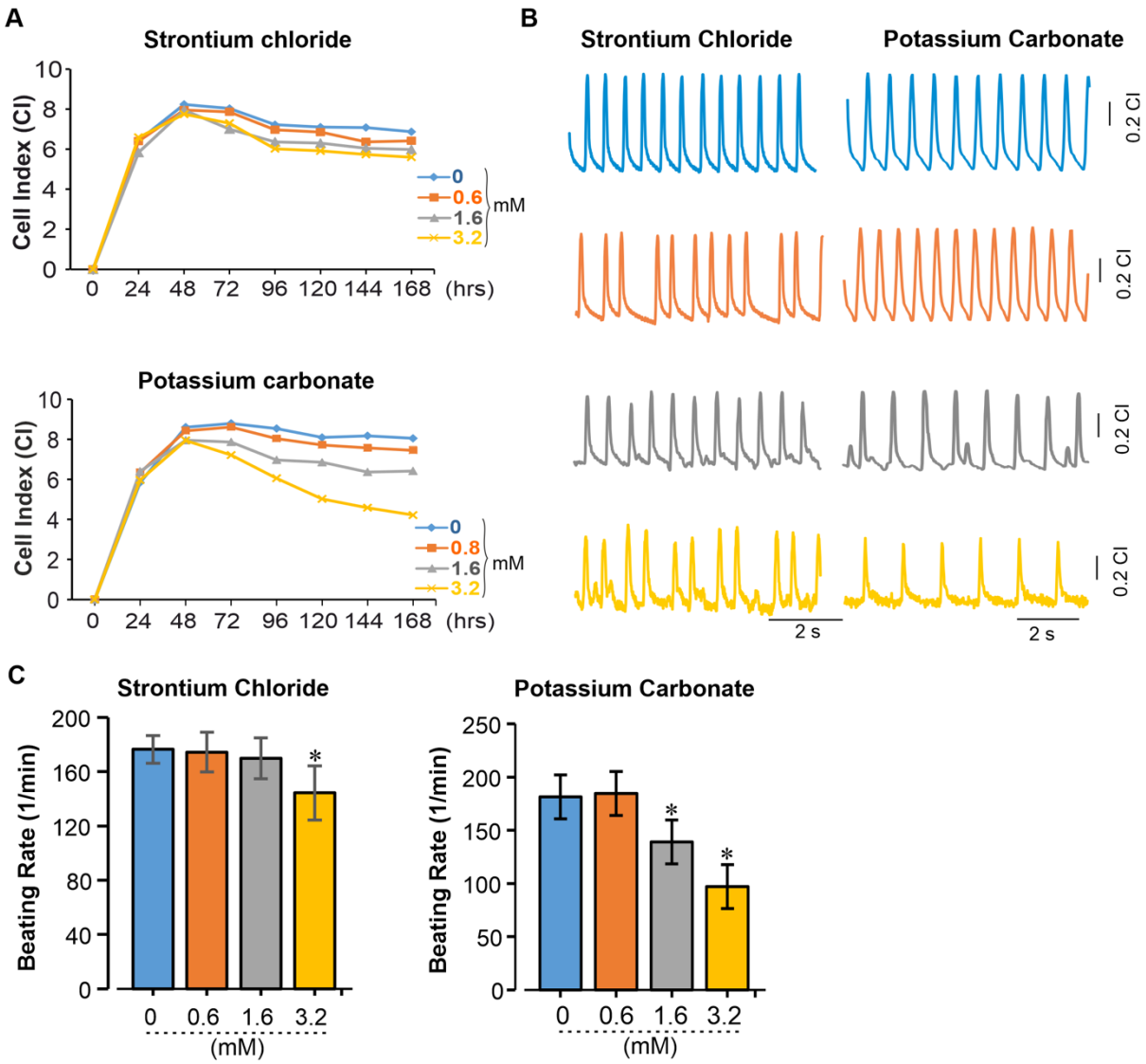

Figure 9. Functional assessment of iPSC-CMs after $SrCl_2$ and K_2CO_3 exposure using the RTCA Cardio System: A. CI traces of iPSC-CMs treated with increasing concentrations of $SrCl_2$ (top) and K_2CO_3 (bottom) over 168 hours. While low and intermediate concentrations (0.6 and 1.6 mM) maintained stable CI values comparable to controls, 3.2 mM induced a gradual decline in CI, more pronounced with K_2CO_3, indicating compound- and dose-dependent cytotoxicity. **B.** Representative beating profiles recorded from iPSC-CMs under treatment with $SrCl_2$ (left) and K_2CO_3 (right). At 3.2 mM, both compounds reduced beating amplitude and regularity, with K_2CO_3 causing more severe arrhythmic and low-amplitude contractions. **C.** Quantification of beating frequency after 168 hours of treatment. While $SrCl_2$ (left) caused a significant reduction in beating rate only at 3.2 mM (p 0.05), K_2CO_3 (right) induced a concentration-dependent decline beginning at 1.6 mM, confirming stronger cardio depressive effects at lower thresholds.

4.4. Field potential Alterations of iPSC-CMs Induced by $SrCl_2$- and K_2CO_3

To investigate the electrophysiological effects of $SrCl_2$ and K_2CO_3 on iPSC-CMs, MEA recordings (**Figure 10A**) were performed following compound exposure. After successful cardiac differentiation and attachment of purified beating clusters to MEA chips, field potential recordings were conducted under increasing compound concentrations. Treatment with $SrCl_2$ resulted in stable field potential traces across intermediate tested concentrations (0.2 – 0.6 mM), showing no apparent alterations in beating frequency or spike morphology (**Figure 10B**). However, treatment with higher concentrations (1.6 – 3.2 mM) caused noticeable changes in both parameters. In contrast, treatment with 3.2 mM K_2CO_3 led to visually reduced field potential amplitude and less defined spike morphology, indicating a possible early cardio depressive effect (**Figure 10C**).

Quantitative MEA analysis supported these observations, beating frequency showed higher variability across concentrations, including both increases and decreases compared to control (**Figure 10D, F**), but a dose-dependent reduction in spike amplitude was observed consistently at 1.6 mM to 3.2 mM for both compounds (**Figure 10E, G**).

Overall, MEA data suggest that $SrCl_2$ and K_2CO_3 exhibit minimal impact on iPSC-CM electrophysiology at low concentrations, whereas higher concentrations of both compounds led to significant disturbances in contractile dynamics, particularly in spike amplitude.

These findings support the notion, that K_2CO_3 may exert cardiotoxic effects at the functional level even in the absence of gross cytotoxicity, emphasizing the importance of functional assays in toxicity screening.

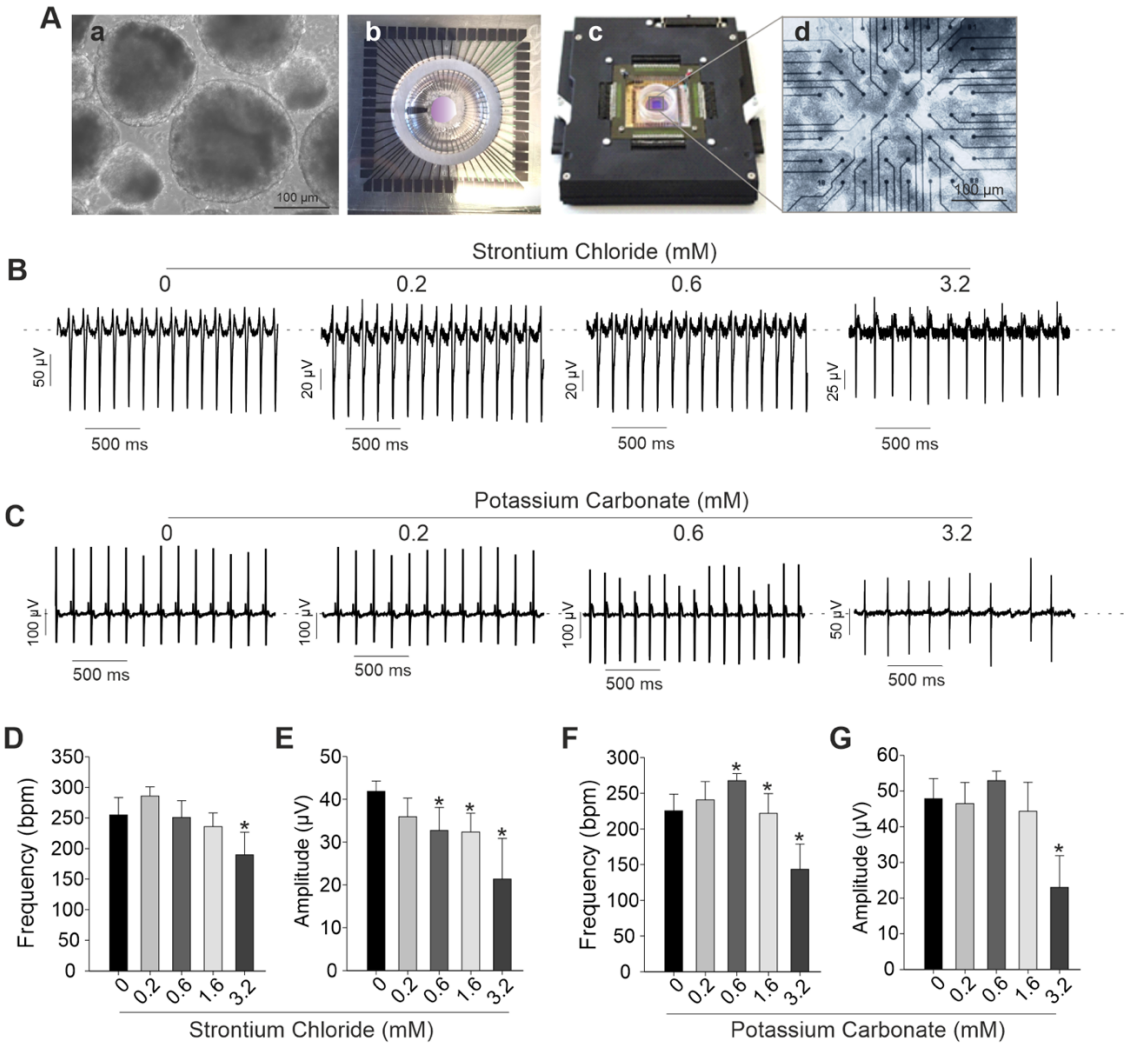

Figure 10. Electrophysiological evaluation of iPSC-CMs after exposure to $SrCl_2$ and K_2CO_3 using MEA technology: A. Overview of the experimental setup used for MEA-based analysis. **a.** Brightfield image of an EB aggregate at day 12 of differentiation. **b-d.** Visualization of the MEA chip and amplifier system used for FP recordings. **B, C.** Representative FP traces illustrating the effect of increasing concentrations of **B.** $SrCl_2$ and **C.** K_2CO_3 on iPSC-CMs function. Changes in spontaneous beating frequency and FP amplitude were observed across the concentration range of 0-3.2 mM. **D, E.** Quantification of spontaneous **D.** beating frequency and **E.** FP amplitude following $SrCl_2$ treatment. A beating significant reduction in frequency was detected at 3.2 mM. FP amplitude showed a significant decrease at concentrations ≥ 0.2 mM. **F, G.** Quantification of electrophysiological responses following K_2CO_3 treatment. **F.** Low doses (0.2-0.6 mM) led to a significant increase in beating frequency, whereas 3.2 mM caused a pronounced reduction. **G.** Similarly, FP amplitude was significantly reduced at 3.2 mM. All values are expressed as mean ± SEM (n= 3-4 independent experiments).

4.5. Gene Expression Analysis of $SrCl_2$ and K_2CO_3 Effects via qRT-PCR

To evaluate the molecular impact of $SrCl_2$ and K_2CO_3 on cardiomyocyte-specific gene expression, qRT-PCR was performed targeting early differentiation markers (*Mesp1*), structural genes (*Myl2, Myh6, MLC2V*), functional ion channel genes (*Scn5a, Cacna1c, Kcnh2*), and the cardiac stress marker *Nppa*. Gene expression was analyzed after 24 h and 72 h of exposure to low and high concentrations of both compounds (0.2 mM and 3.2 mM).

K_2CO_3 induced widespread transcriptional changes in a concentration- and time-dependent manner (**Figure 11A**). Early mesoderm marker (*Mesp1*) expression was markedly suppressed at both concentrations after 24 h, and remained low after 72 h, indicating sustained inhibition of mesodermal lineage signaling. Structural genes showed persistent downregulation. *Myl2* and *Myh6* expression levels were reduced at 24 h and remained consistently suppressed after 72 h, especially at 3.2 mM, suggesting impaired sarcomeric maturation. *Mlc2v* was moderately downregulated at 24 h but recovered toward control levels at 72 h, indicating possible temporal resilience in ventricular lineage identity. Ion channel genes were differentially affected. *Scn5a* showed mild suppression, whereas *Kcnh2* was strongly downregulated at 24 h and remained reduced at 72 h. *Cacna1c* showed moderate but persistent suppression across both time points. The stress marker *Nppa* decreased progressively from 24 to 72 h, supporting a stress-induced phenotype without signs of adaptive compensation.

In contrast, $SrCl_2$ treatment produced more transient and partially reversible transcriptional changes (**Figure 11B**). *Mesp1* expression was reduced after 24 h but recovered to baseline at 72 h, regardless of concentration, suggesting transient disruption of mesodermal signaling. *Myl2* showed slight reductions that remained stable over time, whereas *Myh6* was moderately suppressed at both concentrations without further decline at 72 h. *Mlc2v* exhibited significant downregulation at both time points, particularly at 3.2 mM, indicating sustained effects on ventricular identity. Ion channel gene expression showed only mild reductions. *Scn5a* and *Kcnh2* were slightly decreased at 24 h but recovered by 72 h. *Cacna1c* displayed a similar pattern with transient suppression following normalization. *Nppa* levels decreased at 24 h but partially recovered after 72 h, suggesting limited stress adaptation under $SrCl_2$ treatment.

When comparing both compounds, K_2CO_3 showed more persistent and pronounced suppression of key cardiac genes, particularly in structural (*Myl2, Myh6*), ion channel (*Kcnh2, Scn5a*), and early developmental markers (*Mesp1*), while $SrCl_2$ induced mostly transient effects with partial or full recovery after 72 h. These data suggest distinct transcriptional signatures and time-resolved cellular responses, indicating that K_2CO_3 exerts more consistent transcriptional toxicity in iPSC-CMs than $SrCl_2$.

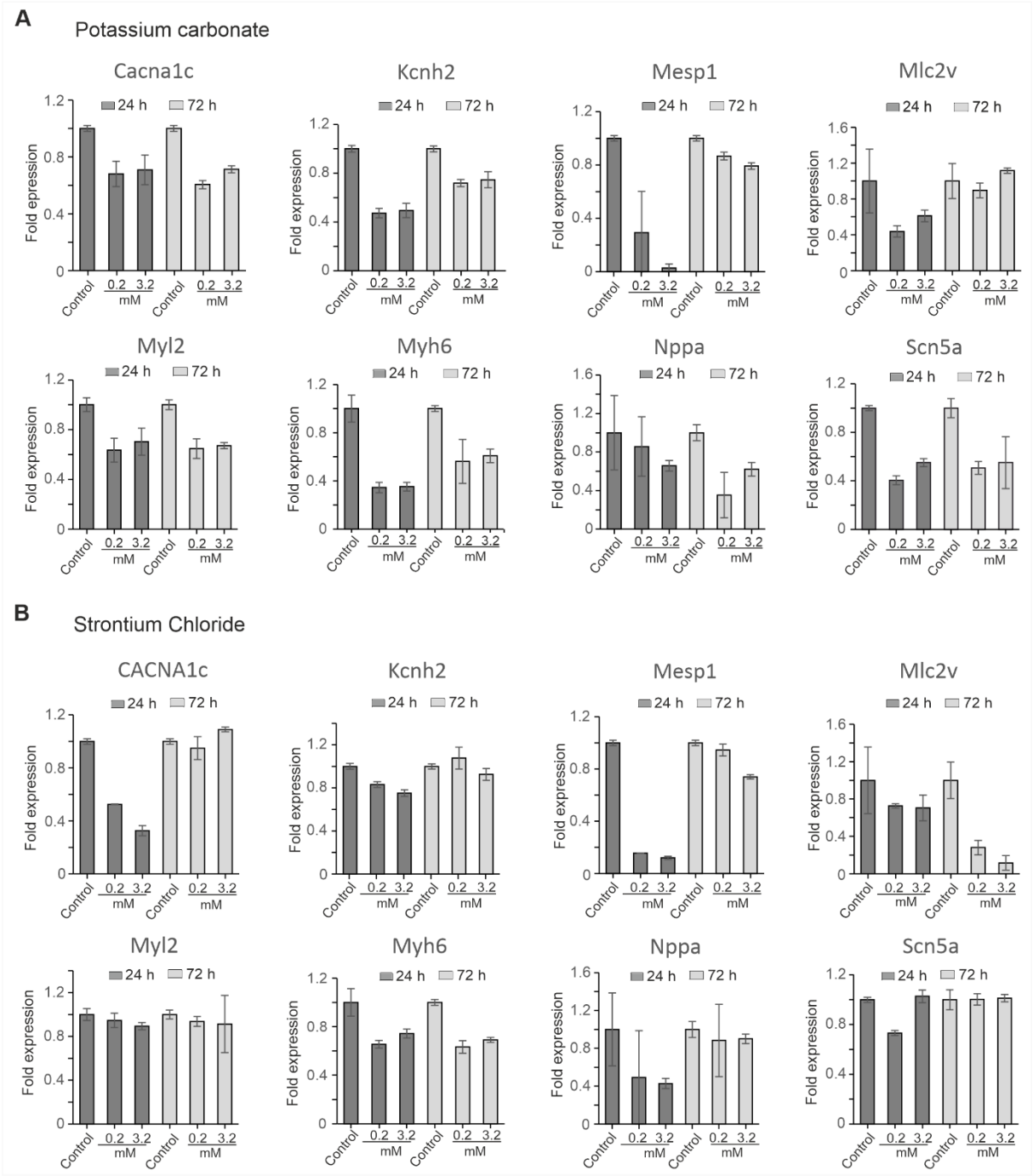

Figure 11. Gene expression analysis of cardiac markers in iPSC-CMs following treatment with $SrCl_2$ and K_2CO_3, as determined by qRT-PCR: A. Expression profiles of selected cardiac genes in iPSC-CMs treated with K_2CO_3 at two concentrations (0.2 mM and 3.2 mM) for 24 and 72 hours, relative to untreated control. The panel includes genes involved in cardiac development and function: the cardiac progenitor marker *Mesp1*, structural markers *Myl2*, *Myh6*, and *Mlc2v*, ion channel genes *Scn5a*, *Cacna1c*, and *Kcnh2*, and the cardiac stress marker *Nppa*. K_2CO_3 exposure resulted in pronounced and sustained downregulation of multiple genes, particularly *Mesp1*, *Myl2*, *Myh6*, and *Kcnh2*, suggesting a disruption

in cardiomyocyte structural integrity and electrophysiological function. **B.** Gene expression patterns following treatment with $SrCl_2$ under identical conditions. Compared to K_2CO_3, $SrCl_2$ induced more transient transcriptional changes. While several genes, including *Mesp1*, *Cacna1c*, and *Kcnh2*, showed initial downregulation at 24 hours, partial or complete recovery was observed by 72 hours, indicating a potentially reversible effect on cardiomyocyte gene expression. All values are presented as mean ± SEM from independent biological replicates.

5. Discussion

In this study, the cardiotoxic and cytotoxic effects of $SrCl_2$ and K_2CO_3 on iPSCs and iPSC-CMs were investigated using a multi-assay approach. The results revealed that both compounds induce significant toxicity in both cell types, evidenced by impaired cell viability, altered electrophysiological function, increased cell death, and changes in cardiac gene expression. $SrCl_2$ exposure led to stimulated iPSC proliferation at some concentrations followed by a measurable reduction in viable CI at higher concentrations and interference in cardiomyocyte beating and electrophysiology. K_2CO_3 exposure, in turn, caused a more consistent disruption of electrical activity, accompanied by a decline in cell viability and proliferation signals, suggesting acute cell detachment or death shortly after exposure. Both compounds triggered cell death pathways as indicated by FACS analysis and induced deregulation of key cardiac mRNA transcripts in qRT-PCR assays; however, partial recovery of gene expression was observed with $SrCl_2$ treatment.

The variable toxicity profile of $SrCl_2$ might likely be due to the chemical similarity of Sr^{2+} to Ca^{2+}, suggesting that mild strontium exposure can mimic calcium dependent signaling and temporarily promote cell growth[134], depending on the cellular context or external factors. This observation aligns with literature reports that strontium salts are not broadly cytotoxic to all cell types at moderate concentrations. For instance, fibroblasts exposed to high levels of $SrCl_2$ (up to 1.25% w/v, approximately 60mM) showed no loss of viability[49]. In that study, $SrCl_2$ did not negatively affect L929 fibroblast cell survival even at concentrations as high as 20% w/v, highlighting that strontium's toxicity is context dependent. In our cardiomyocyte-specific context, however, $SrCl_2$ clearly reduced viable cell numbers over time, implying that excitable, calcium dependent cells like cardiomyocytes are more vulnerable to strontium exposure than fibroblasts.

Our MEA traces showed that $SrCl_2$ exposure at concentrations above 1.6 mM altered spike amplitude and frequency. These findings are consistent with previously described mechanisms in which $SrCl_2$ acts as a calcium analogue, partially substituting for Ca^{2+} and thereby altering intracellular calcium dynamics[134]. Strontium ions can enter cardiomyocytes through L-type calcium channels and substitute for Ca^{2+} in activating the contractile machinery, but their slower kinetics impair repolarization and extend depolarization phases. This incomplete substitution for Ca^{2+} results in prolonged action potential duration, sustained transients of intracellular Ca^{2+} (Sr^{2+}), and arrhythmogenic oscillations. Such electrophysiological disturbances, including extended field potentials and aftercontractions, have been reported in intact cardiac fibers at high Sr^{2+} levels[134,135], supporting our interpretation that $SrCl_2$ can precipitate arrhythmogenic electrical disturbances *in vitro*.

The cardiomyocyte, overwhelmed by aberrant Ca^{2+} signals (or Sr^{2+} signals), activates cell death programs and cannot maintain normal contraction. This mechanism may explain both

the electrical abnormalities (prolonged APS, arrhythmias) and the cell death we observed with $SrCl_2$. It is worth noting that Sr^{2+}'s calcium-mimetic actions can sometimes produce beneficial effects in controlled settings, for example, low concentrations of Sr^{2+} have been reported to promote angiogenesis and reduce cardiomyocyte apoptosis in ischemic cardiac injury models[136], whereas strontium ranelate, an osteoporosis drug, was found to increase cardiovascular risk in some patients, indicating that chronic strontium loading can have adverse cardiac effects[137]. These seemingly paradoxical findings underscore that the dose and context are critical. Small, localized Sr^{2+} releases might pre-condition cells or activate mild stress responses that are cardioprotective.

In addition to its electrical effects, Sr^{2+} is a known agonist of the calcium-sensing receptor (CaSR)[138,139]. Overactivation of CaSR in cardiomyocytes can mobilize Ca^{2+} from intracellular stores via IP_3 signaling, causing excessive Ca^{2+} release from SR and uptake mitochondria. This SR-mitochondrial Ca^{2+} crosstalk triggers mitochondrial membrane potential collapse and the release of apoptogenic factors[140,141]. In a study of hypoxia/reoxygenation injury, CaSR activation was shown to cleave the ER protein BAP31 into a pro-apoptotic fragment, initiating the intrinsic apoptosis pathways in cardiomyocytes[140,141]. By agonizing CaSR, $SrCl_2$ may similarly induce Ca^{2+} release and apoptotic cascades in the cells. Although this mechanism is supported by literature, it was not directly tested in our system and remains a plausible interpretation based on the observed increase in cell death. Mechanistically, the same Sr^{2+}-driven Ca^{2+} stress that provokes chaotic electrical activity in iPSC-CMs is likely to shift Ca^{2+}-dependent cell cycle control in undifferentiated iPSCs, thereby suppressing proliferation.

Beyond calcium mimicry, Sr^{2+} has been shown to modulate signaling pathways such as TGF-β1/2, which can drive angiogenesis via VEGF secretion and RHOA/Rac1 activation[142,143]. While this may be beneficial in regenerative contexts, elevated TGF-β levels in cardiomyocytes are associated with fibrosis and apoptosis, contributing to heart failure progression[144]. Thus, $SrCl_2$'s ability to influence TGF-β signaling may explain both regenerative and pathological outcomes depending on concentration and exposure time.

The exposure to $SrCl_2$ and K_2CO_3 also led to changes in the expression of key cardiac genes, as measured by qRT-PCR. Although detailed gene-by-gene results are beyond scope of this discussion, general patterns were observed that correlate with the functional impairment. For instance, $SrCl_2$-treated cardiomyocytes showed evidence of dysregulated calcium-handling and contractile protein genes. This is plausible given that intracellular Ca^{2+} signaling is a powerful regulator of gene transcription in cardiomyocytes[145]. Disruption of normal Ca^{2+} homeostasis by Sr^{2+} likely triggers maladaptive gene programs, potentially a stress response[141]. It is known from cardiac biology that sustained calcium overload can activate transcription factor such as NFAT or MEF2 via Ca^{2+}/calmodulin-dependent pathways, inducing genes associated with hypertrophy or heart failure[146-148]. In our study, $SrCl_2$ exposure

downregulated adult contractile genes persistently and induced a temporary decrease on stress-associated transcripts, consistent with a cardiotoxic response. While this could suggest activation of cell death pathways, this remains hypothetical, as no specific apoptotic markers were directly assessed. Supporting this, *Hendrych et al.* note that strontium therapy in humans, while beneficial for bones[149,150], is associated with negative cardiac side effects that likely stem from interference in calcium-dependent cardiac processes[137]. Our gene expression findings provide a molecular window into such processes, showing that $SrCl_2$ can alter cardiomyocyte's transcription.

In contrast to $SrCl_2$, K_2CO_3 produced an immediate and mainly inhibitory effect on proliferation, electrophysiological activity, and elevated cell death rates, as confirmed by RTCA and MEA recordings. The toxicity profile is likely dominated by acute ionic imbalance. Excess extracellular K^+ dissipates the transmembrane K^+ gradient, depolarizes the membrane, inactivates voltage-gated Na^+ channels, and thereby prevents action potential initiation[151,152]. This aligns with our MEA data showing noticeable changes in spike amplitude and frequency, indicating acute cytotoxic stress. In practical terms, elevated K^+ rapidly suppresses excitability, similar to the cardiac arrest observed during severe hyperkalemia, including slowed impulse conduction and risk of lethal arrhythmias[151,153-155]. At a resting potential near -80 mV, the inward rectifier K^+ current stabilizes diastole; when external K^+ climbs, the Nernst potential for K^+ becomes less negative, and the resting potential accordingly shifts upward. In our *in vitro* model, the high K^+ load from K_2CO_3 likely brought the murine cardiomyocyte membrane potential closer to 0 mV, effectively silencing the cells by preventing repolarization and re-excitation. Furthermore, depolarization can open some Ca^{2+} channels briefly[156] and, importantly, can reverse the driving force of Na^+/Ca^{2+} exchanger (NCX). Normally, NCX extrudes one Ca^{2+} in exchange for 3 Na^+, using the Na^+ gradient and negative interior as driving force. But if the cell is depolarized to ~-20mV or higher, NCX may operate in reverse. Therefore, sustained depolarization from high K^+ can paradoxically lead to intracellular Ca^{2+} accumulation as well, compounding stress on the cell.

Beyond the electrophysiological matters, K_2CO_3 exposure also resulted in significant gene expression changes, particularly in genes related to cell survival, electrophysiology, and tissue remodeling. Extreme potassium stress is known to activate intracellular signaling cascades (e.g. MAPKs and apoptotic pathways) in cardiomyocytes[154]. Consistent with this, we observed downregulation of genes for normal electrical and contractile function in K_2CO_3-treated cells. In essence, high K_2CO_3 pushes cardiomyocytes into a transcriptional program of cell stress and death, rather than the program for normal beating function. These gene-level disturbances underscore that the toxic impact of K_2CO_3 is not limited to acute electrophysiological arrest; it also includes longer-term changes that could impair recovery even after K^+ normalization.

Furthermore, elevated extracellular potassium has been associated with shifts in cytokine profiles, particularly increased TNF-α and reduced IL-6 expression[157]. These changes could exacerbate cardiac dysfunction, since TNF-α modulates potassium channel activity and promotes apoptotic signaling in cardiomyocytes[158,159], while IL-6 has protective roles in tissue repair and immune regulation. Suppression of IL-6 may impair cardiomyocyte resilience to stress. Notably, studies showed that blocking IL-6 signaling, e.g. via SOCS3, can reduce hypertrophy and apoptosis in cardiac tissue[160], underscoring its regulatory importance. Although we did not assess cytokine levels directly, this literature suggests a possible immunomodulatory effect of high K^+ that may contribute to the observed functional impairment. Taken together, the qRT-PCR data for both compounds highlight that $SrCl_2$ and K_2CO_3 exposures disturb the genetic regulators of cardiomyocyte viability and function, corroborating the results such as reduced contractility and increased cell death.

Although both $SrCl_2$ and K_2CO_3 were toxic to murine cardiomyocytes, their toxicity differed. Several contrasting aspects were evident, K_2CO_3 caused irregular and low amplitude beating and a progressive decline in viability. This acute effect corresponds to the well-known immediate cardioplegic action of high K^+. Clinicians intentionally induce asystole within seconds by perfusing the heart with high K^+ solutions during surgery[154]. On the other side, if high K^+ is removed, electrical activity can resume. So, in our *in vitro* context, if K_2CO_3 was washed out before cells irreversibly died, one might expect partial recovery of beating and viability. In contrast, $SrCl_2$'s effects built up more gradually; it preserved rhythmic contractions at intermediate concentrations, while showing reduced amplitude, frequency, and cell viability at highest concentration. Once Sr^{2+} has entered cells and disrupted Ca^{2+} homeostasis, simply washing it out might not rapidly reverse the apoptotic signaling. Sr^{2+} impact on the action potential was found to be "pronounced and progressive" in Purkinje fibers, not easily reversed except by reintroducing Ca^{2+}[134], suggesting that sustained exposure leads to accumulating dysfunction.

Another aspect of K_2CO_3 is its carbonate component, which makes the solution strongly alkaline. Although our cell culture medium was buffered, a spike of K_2CO_3 could locally raise pH and cause alkaline injury to cells[161]. High pH can denature proteins and cause lipid membrane saponification. The safety data for K_2CO_3 note it is a caustic substance that can cause tissue burns on contact[57,162]. Consistent with the observed changes in morphology and the reduced EB diameter, this caustic effect could have contributed to cell membrane damage.

In summary, $SrCl_2$ and K_2CO_3 probably act through different primary mechanisms, one mimicking calcium and derailing calcium-dependent processes, the other overwhelming potassium homeostasis and extinguishing excitability, yet both mechanisms converge on a common theme: disruption of ionic equilibrium in cardiomyocytes leading to calcium overload, contractile failure, and cell injury. Calcium is central in both cases, directly for Sr^{2+}, indirectly

for K^+, which is not surprising given Ca^{2+}'s role in cardiomyocyte life and death. Such mechanistic distinctions are crucial in toxicological risk assessment and for defining exposure thresholds, particularly when utilizing high-resolution *in vitro* models such as MEA or impedance-based screening platforms, which allow for time- and concentration-resolved profiling of cardiotoxic responses. Although mechanistic pathways such as CaSR activation or membrane depolarization remain speculative within the scope of this study, the combined functional, molecular, and morphological data clearly demonstrate that both $SrCl_2$ and K_2CO_3 exhibit dose-dependent cardiotoxic and cytotoxic effects in iPSCs and iPSC-CMs.

5.1. Limitations of the Present In Vitro Model

While our findings provide valuable insights, it is important to recognize the limitations of this *in vitro* model. First, we utilized murine iPSCs and iPSC-CMs, which may differ from adult human CMs in several respects. Murine CMs have much faster beating rates and significantly shorter action potential durations than human CMs[163,164]. The ion channel expression profile in mice means that their response to ionic perturbations can differ quantitatively from human heart cells[163,165]. Moreover, our in vitro exposures were acute and in an isolated setting. This lacks the contributions of systemic factors present in an intact organism. In a living animal, homeostatic mechanism, and multi-cellular interactions could modulate the effects of $SrCl_2$ and K_2CO_3. Another limitation is that we focused on single-compound exposures. In realistic scenarios, $SrCl_2$ or K_2CO_3 toxicity might occur in the context of other stressors or compounds. For example, $SrCl_2$ or K_2CO_3 might interact with other electrolytes or medications, our controlled experiments do not account for such interactions. Ideally, complementary *in vivo* studies (e.g. in animal models) or human cardiomyocyte experiments would be performed to validate that similar toxicity occurs at relevant doses.

Finally, our readouts (impedance, MEA, FACS, qRT-PCR) provide a broad view of cardiomyocyte health, but each has limitations in sensitivity and specificity although iPSCs and iPSC-CMs provide a valuable model for investigating cellular reactions. There could be subtler effects of $SrCl_2$ or K_2CO_3, such as changes in metabolic activity, oxidative stress level, or electrophysiological heterogeneity that we did not directly measure. These could be explored in future studies using assays for ATP content, reactive oxygen species, or high-resolution mapping of conduction, respectively. In summary, caution is warranted in translating these *in vitro* results to *in vivo* cardiac risk. The model is extremely useful for mechanistic understanding and relative comparison of toxicity, but factors like species differences, cell maturity, systemic responses, and dose extrapolation must be considered.

In addition, while our study assessed acute effects, the chronic toxicity of $SrCl_2$ and K_2CO_3 remains underexplored. Long-term exposure may involve additional mechanism of damage, including inflammatory signaling and epigenetic modulation. Future research should therefore

explore the sustained, low-dose impact of these compounds on cardiac tissue, ideally integrating molecular profiling and *in vivo* validation studies.

5.2. Potential Implications for Clinical Practice

Despite the above limitations, our findings carry important implications for toxicological screening and compound safety assessments in both medical and industrial contexts. iPSC-CMs have emerged as a powerful tool for preclinical cardiotoxicity testing. The distinct profile observed for $SrCl_2$ or K_2CO_3 in our study illustrate why a multi-parametric screening approach is crucial. Comprehensive screening can detect both functional cardiotoxicity (e.g. arrhythmias, contractile failure) and structural cardiotoxicity (cell death, molecular damage). From a regulatory perspective, the results underscore that even seemingly simple inorganic compounds can have complex cardiotoxic effects. This is particularly relevant in vulnerable populations, such as children, pregnant women, or individuals with impaired cognitive or renal function, who may unintentionally ingest or accumulate higher doses of these substances. Such cases illustrate the need for heightened awareness and education regarding potential risks associated with over the counter and oral care products. $SrCl_2$ or K_2CO_3 are not typical "drug-like" molecules, yet their impact on heart cells is profound. This suggests that industries handling such compounds, should be mindful of potential cardiac risk in cases of accidental exposure. Safety protocols must consider cardiotoxic endpoints. Our study also has implications for environmental health. Sr^{2+} is a trace element sometimes found in groundwater or released in certain industrial effluents[39-43], and K_2CO_3 can be a component of industrial waste[53-56]. Environmental toxicology assessments could utilize cardiomyocyte assays to gauge if such contaminants pose a risk to cardiac function in wildlife or humans, for example, if drinking water contamination occurred.

Finally, our results highlight the importance of using human-relevant cell systems in safety testing. While we used murine iPSCs and iPSC-CMs, the approach can be readily applied to human iPSC-CMs, which are increasingly used in safety pharmacology and could strengthens the evidence that these substances would be hazardous to human cardiac health. The toxicological behavior of $SrCl_2$ or K_2CO_3 resembles recent examples from regulatory toxicology, where common cosmetic ingredient such as triclosan, titanium dioxide, or sodium lauryl sulfate were shown to impair proliferation, induce inflammation, or delay tissue regeneration in human cell models[166-170]. These precedents highlight how even long-established substances can have unexpected cytotoxic or cardiotoxic effects when reassessed using modern cell-based assays[171-180].

Given their wide applicability and biological potency, both $SrCl_2$ and K_2CO_3 should be re-evaluated in the context of modern toxicological setting. A balance must be struck between

their functional utility and the potential cellular risks they pose, especially to excitable tissues such as the heart.

6. References

1. Cvikl B, Lussi A, Gruber R. The in vitro impact of toothpaste extracts on cell viability. *European Journal of Oral Sciences* 2015; **123 (3)**: 179-85.
2. Weber T. Memorix Zahnmedizin. Stuttgart: Thieme; 2017.
3. Saxton CA, Harrap GJ, Lloyd AM. The effect of dentifrices containing zinc citrate on plaque growth and oral zinc levels. *Journal of Clinical Periodontology* 1986; **13 (4)**: 301-6.
4. Bellamy PG, Khera N, Day TN, Mussett AJ, Barker ML. A randomized clinical study comparing the plaque inhibition effect of a SnF2/SHMP dentifrice (blend-a-med EXPERT GUMS PROTECTION) and a chlorhexidine digluconate dentifrice (Lacalut Aktiv). *The Journal of clinical dentistry* 2009; **20 (2)**: 33-8.
5. Sowinski J, Battista G, Petrone DM, et al. A twelve-week clinical comparison of two tartar control dentifrices. *Journal of Clinical Dentistry* 2000; **11 (3)**: 76-9.
6. Anwar MA, Sayed GA, Hal DM, et al. Herbal remedies for oral and dental health: a comprehensive review of their multifaceted mechanisms including antimicrobial, anti-inflammatory, and antioxidant pathways. *Inflammopharmacology* 2025; **33 (3)**: 1085-160.
7. Sieckmann C. Zur antimikrobiellen Wirkung von Zahnpasten (Dissertation). 2014. https://www.db-thueringen.de/receive/dbt_mods_00023591 (accessed 09/11/ 2022).
8. Kellar KE, Nicinska J, inventors; USE OF SODIUM DECYL SULFATE IN TOOTHPASTE. United States patent US 2006/0093562 A1. 2004.
9. Colgate Palmolive Company, inventor Dentifrice compositions containing reactive ingredients stabilized with alkali metal compounds. United States patent US 5,565,190. 1994.
10. Axelsson P, D O. Concept and practice of plaque-control. *The American Academy of Pedodontics* 1981; **3**(Special Issue): 101-13.
11. Umbach W. Kosmetik und Hygiene von Kopf bis Fuß. Weinheim: Wiley-VCH; 2004.
12. Bossù M, Saccucci M, Salucci A, et al. Enamel remineralization and repair results of Biomimetic Hydroxyapatite toothpaste on deciduous teeth: an effective option to fluoride toothpaste. *Journal of Nanobiotechnology* 2019; **17 (17)**.
13. Schiffner U. Verwendung von Fluoriden zur Kariesprävention. *Bundesgesundheitsblatt Gesundheitsforschung Gesundheitsschutz* 2021; **64 (7)**: 830–7.
14. Nordström A, Birkhed D. Preventive Effect of High-Fluoride Dentifrice (5,000 ppm) in Caries-Active Adolescents: A 2-Year Clinical Trial. *Caries Research* 2010; **44 (3)**: 323-31.

15. Hobbs M, Marek L, Clarke R, et al. Investigating the prevalence of non-fluoride toothpaste use in adults and children using nationally representative data from New Zealand: a cross-sectional study. *British Dental Journal* 2020; **228 (4)**: 269–76.
16. Chen J, Ahmad R, Li W, Swain M, Li Q. Biomechanics of oral mucosa. *Journal of The Royal Society Interface* 2015; **12 (109)**: 1-20.
17. BfVu, Bundesamt für Verbraucherschutz und Lebensmittelsicherheit. Gesetzliche Regelungen bei Inhaltsstoffen. 2023. https://www.bvl.bund.de/DE/Arbeitsbereiche/03_Verbraucherprodukte/03_AntragstellerUnternehmen/02_Kosmetik/04_Inhaltsstoffe/bgs_fuerAntragsteller_kosmetik_gesetzlicheRegelung_inhaltsstoffe_node.html (accessed 01/27/ 2024).
18. SCCP, Scientific Committee on Consumer Products. The SCCP'S Notes of Guidance for the testing of cosmetic ingredients and their safety evaluation. 2006. https://ec.europa.eu/health/ph_risk/committees/04_sccp/docs/sccp_o_03j.pdf (accessed 01/27/ 2024).
19. FDA, Food and Drug Administration. CFR - Code of Federal Regulations Title 21. 2022. https://www.accessdata.fda.gov/scripts/cdrh/cfdocs/cfcfr/cfrsearch.cfm?fr=355.50 (accessed 09/17/ 2022).
20. Europäische Kommission. Verordnung (EU) Nr. 358/2014 DER KOMMISSION. 2014. https://eur-lex.europa.eu/legal-content/DE/TXT/PDF/?uri=CELEX:32014R0358&from=DE (accessed 09/16/ 2022).
21. FDA, Food and Drug Administration. 5 Things to Know About Triclosan. 2019. https://www.fda.gov/consumers/consumer-updates/5-things-know-about-triclosan (accessed 09/16/ 2022).
22. Flechsig T. Titandioxid in Zahnpasten. 2021. https://www.zahnarzt-flechsig.de/titandioxid-in-zahnpasten (accessed 10/28/ 2025).
23. EFSA, European Food Safety Authority. Titanium dioxide: E171 no longer considered safe when used as a food additive. 2021. https://www.efsa.europa.eu/en/news/titanium-dioxide-e171-no-longer-considered-safe-when-used-food-additive (accessed 09/16/ 2022).
24. BfR, Bundesinstitut für Risikobewertung. Titandioxid - gibt es gesundheitliche Risiken? 2021. https://www.bfr.bund.de/de/titandioxid___gibt_es_gesundheitliche_risiken_-240812.html (accessed 09/16/ 2022).
25. Kirkland D, Aardema MJ, Battersby RV, et al. A weight of evidence review of the genotoxicity of titanium dioxide (TiO2). *Regulatory Toxicology and Pharmacology* 2022; **136 (105263)**.
26. EMA, European Medicines Agency. Background review for sodium laurilsulfate used as an excipient. 2015. https://www.ema.europa.eu/en/documents/report/background-

review-sodium-laurilsulfate-used-excipient-context-revision-guideline-excipients-label_en.pdf (accessed 09/16/ 2022).

27. Herlofson BB, Barkvoll P. The effect of two toothpaste detergents on the frequency of recurrent aphthous ulcers. *Acta Odontologica Scandinavica* 1996; **54 (3)**: 150-3.
28. Haleon. Sensodyne Original. 2022. https://www.sensodyne-me.com/en_AE/products/original-toothpaste.html (accessed 06/14/ 2025).
29. Snow Pearl GmbH. Pearl Shield Plus Fluoride Gel Zahnpasta. 2021. https://snow-pearl.com/en/products/pearl-shield-plus-gel-zahnpasta-75-ml?srsltid=AfmBOoq_3y8-l-IuWbjGsT6U8oaZ14tC6AwPutRBwaVtFMcGg8LUWnwB#:~:text=COMPOSITION (accessed 06/15/ 2025).
30. theraphango. Pflegende Fango Zahncreme 2025. https://theraphango.com/en/products/medizinische-zahncreme?srsltid=AfmBOormr0QG7iFz-3TADit_YwmaosNQ7HDtad8NJ7iE0LjNo8To3WQo#:~:text=Complete%20declaration%20of%20ingredients%3A (accessed 06/15/ 2025).
31. Serumwerk Bernburg AG. Parodontal® Mundsalbe. 2021. https://parodontal.de/parodontal-2/#inhaltsstoffe (accessed 06/15/ 2025).
32. medindia. Holistic Doctor Launches ALKA-WHITE® The Revolutionary Alkaline Oral Cleanse™. 2019. https://www.medindia.net/health-press-release/holistic-doctor-launches-alka-white-the-revolutionary-alkaline-oral-cleanse-422147-1.htm (accessed 06/13/ 2025).
33. VuMA, Verbrauchs- und Medienanalyse. Umfrage zur Häufigkeit der Verwendung von sensitiver Zahnpasta bis 2021. 2021. https://de.statista.com/statistik/daten/studie/181209/umfrage/haeufigkeit-verwendung-von-sensitiver-zahncreme-oder-zahngel/ (accessed 09/12/ 2022).
34. Arshad S, Zaidi SJA, Farooqui WA. Comparative efficacy of BioMin-F, Colgate Sensitive Pro-relief and Sensodyne Rapid Action in relieving dentin hypersensitivity: a randomized controlled trial. *BMC Oral Health* 2021; **21 (1)**: 498.
35. ChemSpider. Strontium chloride. 2025. https://www.chemspider.com/Chemical-Structure.55440.html (accessed 10/28/ 2025).
36. Pinto SCS, Silveira CMM, Pochapski MT, Pilatti GL, Santos FA. Effect of desensitizing toothpastes on dentin. *Brazilian Oral Research* 2012; **26 (5)**: 410-7.
37. Lippert F. The effects of fluoride, strontium, theobromine and their combinations on caries lesion rehardening and fluoridation. *Archives of Oral Biology* 2017; **80**: 217-21.
38. Alencar CdM, Pedrinha VF, Araújo JLN, Esteves RA, da Silveira ADS, Silva CM. Effect of 10% Strontium Chloride and 5% Potassium Nitrate with Fluoride on Bleached Bovine Enamel. *The Open Dentistry Journal* 2017; **11**: 476-84.

39. Dufter-Münster AMW, Harter AG, Klapötke TM, Reinhardt E, Römer J, Stierstorfer Jr. Lithium Nitropyrazolates as Potential Red Pyrotechnic Colorants. *European Journal of Inorganic Chemistry* 2022; **2022 (8)**: e202101048.
40. Dufter AMW, Klapötke TM, Rusan M, Schweiger A, Stierstorfer J. Comparison of Functionalized Lithium Dihydrobis(azolyl)borates with Their Corresponding Azolates as Environmentally Friendly Red Pyrotechnic Coloring Agents. *ChemPlusChem* 2020; **85 (9)**: 2044-50.
41. Fengqin L, Kuangdi X. Strontium Metallurgy. In: Xu K, ed. The ECPH Encyclopedia of Mining and Metallurgy. Beijing: Springer, Singapore; 2023: 978-81.
42. Denry I, Goudouri O-M, Harless JD, Hubbard EM, Holloway JA. Strontium-releasing fluorapatite glass-ceramics: crystallization behavior, microstructure and solubility. *Journal of Biomedical Materials Research Part B: Applied Biomaterials* 2018; **106 (4)**: 1421–30.
43. NEMI. USGS-NWQL: I-1800: Strontium, dissolved, atomic absorption spectrometric2002. https://www.nemi.gov/methods/method_summary/5475/ (accessed 06/11/2025).
44. Kishore A, Mehrotra KK, Saimbi CS. Effectiveness of Desensitizing Agents. *Journal of Endodontics* 2002; **28 (1)**: 34-5.
45. Liu H, Hu D. Efficacy of a Commercial Dentifrice Containing 2% Strontium Chloride and 5% Potassium Nitrate for Dentin Hypersensitivity: A 3-Day Clinical Study in Adults in China. *Clinical Therapeutics* 2012; **34 (3)**: 614-22.
46. Hahn GS. Strontium Is a Potent and Selective Inhibitor of Sensory Irritation. Dermatologic Surgery. 1999:689-94.
47. LUMITOS AG. Strontiumchlorid. 2025. https://www.chemie.de/lexikon/strontiumchlorid.html (accessed 06/11/ 2025).
48. Nightengale B, Brune M, Blizzard SP, Ashley-Johnson M, Slan S. Strontium chloride Sr 89 for treating pain from metastatic bone disease. *American Journal of Health-System Pharmacy* 1995; **52 (20)**: 2189-95.
49. Akyol M, Polat ZA, Özçelik S, Kaya Oz. The effects of strontium chloride on viability of mouse connective tissue fibroblast cells. *Cumhuriyet Medical Journal* 2013; **35 (1)**: 33-8.
50. Pasqualetti S, Banfi G, Mariotti M. The effects of strontium on skeletal development in zebrafish embryo. *Journal of Trace Elements in Medicine and Biology* 2013; **27 (4)**: 375-9.
51. Romagnoli C, Zonefrati R, Galli G, et al. The effect of strontium chloride on human periodontal ligament stem cells. *Clinical Cases in Mineral and Bone Metabolism* 2017; **14 (3)**: 283-93.

52. Atrash S, Gross L. The Effect of Alka-White Mint and Alka-White Turmeric on the Oral Cavity. 2017. https://www.ecronicon.com/ecde/pdf/ECDE-07-0000225.pdf (accessed 09/12/ 2022).
53. Lengheim H, inventor Verfahren zur Herstellung von Kaliumkarbonat. Austria/Wien patent EP 3 431 441 A1. 2019.
54. Ma DH, Jaladi AK, Lee JH, et al. Catalytic Hydroboration of Aldehydes, Ketones, and Alkenes Using Potassium Carbonate: A Small Key to Big Transformation. *ACS Omega* 2019; **4 (14)**: 15893−903.
55. Lang A. Kalium carbonicum: Schonende Hilfe nach Wehen und Geburt. 2018. https://www.lifeline.de/therapien/homoeopathie/wirkstoffe/kalium-carbonicum-id166723.html (accessed 09/12/ 2022).
56. Pascoe. Naturmedizinischer Wirkstoff Kaliumcarbonat. 2022. https://www.pascoe.de/wirkstoffe/detail/kaliumcarbonat.html (accessed 09/12/ 2022).
57. Cosmetic Ingredient Review. Safety Assessment of Carbonate Salts as Used in Cosmetics. 2016. https://www.cir-safety.org/supplementaldoc/safety-assessment-carbonate-salts-used-cosmetics (accessed 06/1/ 2019).
58. Akintunde JK, Opeolu BO, Aina OO. Exposure to potassium carbonate emulsion induced nephro-toxicity in experimental animals. *Jordan Journal of Biological Sciences* 2010; **3 (2)**: 65-8.
59. Bui QQ, Clark CR, Naas DJ, Ulrich CE, Elangbam CS. A subacute inhalation exposure evaluation of a scrubbing solution used in petroleum refineries. *Journal of Toxicology and Environmental Health A* 1998; **54 (1)**: 49-62.
60. Lastauskiene E, Zinkeviciene A, Girkontaite I, Kaunietis A, Kvedariene V. Formic Acid and Acetic Acid Induce a Programmed Cell Death in Pathogenic Candida Species. *Current Microbiology* 2014; **69 (3)**: 303-10.
61. Kolios G, Moodley Y. Introduction to Stem Cells and Regenerative Medicine. *Respiration* 2013; **85 (1)**: 3-10.
62. Zakrzewski W, Dobrzyński M, Szymonowicz M, Rybak Z. Stem cells: past, present, and future. *Stem Cell Research & Therapy* 2019; **10 (1)**: 68.
63. Evans MJ, Kaufman MH. Establishment in culture of pluripotential cells from mouse embryos. *Nature* 1981; **292**: 154-6.
64. Robey PG. Cell Sources for Bone Regeneration: The Good, the Bad, and the Ugly (But Promising). *Tissue Engineering Part B* 2011; **17(6)**: 423-30.
65. Thomson JA, Itskovitz-Eldor J, Shapiro SS, et al. Embryonic Stem Cell Lines Derived from Human Blastocysts. *SCIENCE* 1998; **282 (5391)**: 1145-7.
66. Condic ML, Rao M. Alternative Sources of Pluripotent Stem Cells: Ethical and Scientific Issues Revisited. *Stem Cells and Development* 2010; **19 (8)**: 1121-9.

67. Laschinski G, Vogel R, Spielmann H. Cytotoxicity test using blastocyst-derived euploid embryonal stem cells: a new approach to in vitro teratogenesis screening. *Reproductive Toxicology* 1991; **5 (1)**: 57-64.
68. Sehlmeyer U, Meister A, Beisker W, Wobus AM. Low mutagenic effects of mitomycin C in undifferentiated embryonic P19 cells are correlated with efficient cell cycle control. *Mutation Research/Fundamental and Molecular Mechanisms of Mutagenesis* 1996; **354 (1)**: 103-12.
69. Scholz G, Pohl I, Genschow E, Klemm M, Spielmann H. Embryotoxicity Screening Using Embryonic Stem Cells in vitro: Correlation to in vivo Teratogenicity. *Cells Tissues Organs* 1999; **165 (3-4)**: 203–11.
70. O'Shea KS. Directed differentiation of embryonic stem cells: genetic and epigenetic methods. *Wound Repair and Regeneration* 2001; **9 (6)**: 443-59.
71. Herberts CA, Kwa MS, Hermsen HP. Risk factors in the development of stem cell therapy. *Journal of Translational* 2011; **9 (29)**: 1-14.
72. Kent L. Culture and Maintenance of Human Embryonic Stem Cells. *Journal of Visualized Experiments* 2009; **34 (1427)**.
73. Takahashi K, Yamanaka S. Induction of Pluripotent Stem Cells from Mouse Embryonic and Adult Fibroblast Cultures by Defined Factors. *Cell* 2006; **126 (4)**: 663–76.
74. Kim JB, Greber B, Arauzo-Bravo MJ, et al. Direct reprogramming of human neural stem cells by OCT4. *Nature* 2009; **461**: 649-53.
75. Scarfone RA, Pena SM, Russell KA, Betts DH, Koch TG. The use of induced pluripotent stem cells in domestic animals: a narrative review. *BMC Veterinary Research* 2020; **16**: 477.
76. Anson BD, Kolaja K, Kamp TJ. Opportunities for Human iPS Cells in Predictive Toxicology. *Clinical Pharmacology & Therapeutics* 2011; **89 (5)**: 754-8.
77. Marchetto MCN, Carromeu C, Acab A, et al. A model for neural development and treatment of Rett Syndrome using human induced pluripotent stem cells. *Cell* 2010; **143 (4)**: 527-39.
78. Fatima A, Xu G, Nguemo F, et al. Murine transgenic iPS cell line for monitoring and selection of cardiomyocytes. *Stem Cell Research* 2016; **17 (2)**: 266-72.
79. Sobhani A, Khanlarkhani N, Baazm M, et al. Multipotent Stem Cell and Current Application. *Acta Medica Iranica* 2017; **55 (1)**: 6-23.
80. Parrotta EI, Lucchino V, Scaramuzzino L, Scalise S, Cuda G. Modeling Cardiac Disease Mechanisms Using Induced Pluripotent Stem Cell-Derived Cardiomyocytes: Progress, Promises and Challenges. *International Journal of Molecular Sciences* 2020; **21 (12)**: 4354.

81. Csöbönyeiová Mr, Polák St, Danišovic Lu. Toxicity testing and drug screening using iPSC-derived hepatocytes, cardiomyocytes, and neural cells. *Canadian Journal of Physiology and Pharmacology* 2016; **94**: 687-94.
82. Passier R, Oostwaard DW, Snapper J, et al. Increased Cardiomyocyte Differentiation from Human Embryonic Stem Cells in SerumFree Cultures. *Stem Cells* 2005; **23**: 772-80.
83. Osafune K, Caron L, Borowiak M, et al. Marked differences in differentiation propensity among human embryonic stem cell lines. *Nature Biotechnology* 2008; **26 (3)**: 313-5.
84. Burridge PW, Matsa E, Shukla P, et al. Chemically defined generation of human cardiomyocytes. *Nature Methods* 2014; **11 (8)**: 855-60.
85. Kaichi S, Hasegawa K, Takaya T, et al. Cell line-dependent differentiation of induced pluripotent stem cells into cardiomyocytes in mice. *Cardiovascular Research* 2010; **88**: 314-23.
86. Kehat I, Kenyagin-Karsenti D, Snir M, et al. Human embryonic stem cells can differentiate into myocytes with structural and functional properties of cardiomyocytes. *Journal of Clinical Investigation* 2001; **108 (3)**: 407–14.
87. Karakikes I, Ameen M, Termglinchan V, Wu JC. Human Induced Pluripotent Stem Cell-Derived Cardiomyocytes: Insights into Molecular, Cellular, and Functional Phenotypes. *Circulation Research* 2015; **117 (1)**: 80–8.
88. Hartman ME, Dai D-F, Laflamme MA. Human Pluripotent Stem Cells: Prospects and Challenges as a Source of Cardiomyocytes for In Vitro Modeling and Cell-Based Cardiac Repair. *Advanced Drug Delivery Reviews* 2016; **96**: 3–17.
89. Yang X, Pabon L, Murry CE. Engineering Adolescence: Maturation of Human Pluripotent Stem Cell-derived Cardiomyocytes. *Circulation Research* 2014; **114 (3)**: 511–23.
90. Veerman CC, Kosmidis G, Mummery CL, Casini S, Verkerk AO, Bellin M. Immaturity of Human Stem-Cell-Derived Cardiomyocytes in Culture: Fatal Flaw or Soluble Problem? *Stem Cells and Development* 2015; **24 (9)**: 1035-52.
91. Gupta MK, Illich DJ, Gaarz A, et al. Global transcriptional profiles of beating clusters derived from human induced pluripotent stem cells and embryonic stem cells are highly similar. *BMC Developmental Biology* 2010; **10**: 98.
92. Yokoo N, Baba S, Kaichi S, et al. The effects of cardioactive drugs on cardiomyocytes derived from human induced pluripotent stem cells. *Biochemical and Biophysical Research Communications* 2009; **387 (3)**: 482-8.
93. Bédard P, Gauvin S, Ferland K, et al. Innovative Human Three-Dimensional Tissue-Engineered Models as an Alternative to Animal Testing. *bioengineering* 2020; **7 (3)**: 115.

94. Reddy N, Lynch B, Gujral J, Karnik K. Alternatives to animal testing in toxicity testing: Current status and future perspectives in food safety assessments. *Food and Chemical Toxicology* 2023; **179**: 113944.
95. Westfall A, Sigurdson GT, Rodriguez-Saona LE, Giusti MMn. Ex Vivo and In Vivo Assessment of the Penetration of Topically Applied Anthocyanins Utilizing ATR-FTIR/PLS Regression Models and HPLC-PDA-MS. *Antioxidants* 2020; **9 (6)**: 486.
96. Xu Y, Shrestha N, Préat V, Beloqui A. An overview of in vitro, ex vivo and in vivo models for studying the transport of drugs across intestinal barriers. *Advanced Drug Delivery Reviews* 2021; **175**: 113795.
97. He S, Zhang X, Lu S, Zhu T, Sun G, Sun X. A Computational Toxicology Approach to Screen the Hepatotoxic Ingredients in Traditional Chinese Medicines: Polygonum multiflorum Thunb as a Case Study. *Biomolecules* 2019; **9 (10)**: 577.
98. Nigsch F, Macaluso NM, Mitchel JB, Zmuidinavicius D. Computational toxicology: an overview of the sources of data and of modelling methods. *Expert Opinion on Drug Metabolism & Toxicology* 2009; **5 (1)**: 1-14.
99. Luker T, Alcaraz L, Chohan KK, et al. Strategies to improve in vivo toxicology outcomes for basic candidate drug molecules. *Bioorganic & Medicinal Chemistry Letters* 2011; **21 (19)**: 5673–9.
100. Peters J-U, Schnider P, Mattei P, Kansy M. Pharmacological Promiscuity: Dependence on Compound Properties and Target Specificity in a Set of Recent Roche Compounds. *ChemMedChem* 2009; **4 (4)**: 680 – 6.
101. Price DA, Blagg J, Jones L, Greene N, Wager T. Physicochemical drug properties associated with in vivotoxicological outcomes: a review. *Expert Opinion on Drug Metabolism & Toxicology* 2009; **5 (8)**: 921-31.
102. Kavlock R, Chandler K, Houck K, et al. Update on EPA's ToxCast Program: Providing High ThroughputDecision Support Tools for Chemical Risk Management. *Chemical Research in Toxicology* 2012; **25 (7)** 1287–302.
103. Ford KA. Refinement, Reduction, and Replacement of Animal Toxicity Tests by Computational Methods. *ILAR Journal* 2016; **57 (2)** 226–33.
104. Judson RS, Houck KA, Kavlock RJ, et al. In Vitro Screening of Environmental Chemicals for Targeted Testing Prioritization: The ToxCast Project. *Environmental Health Perspectives* 2010; **118 (4)**: 485-92.
105. Low Y, Sedykh A, Golbraikh A, Whelan M, Rusyn I, Tropsha A. Integrative Chemical−Biological Read-Across Approach for ChemicalHazard Classification. *Chemical Research Toxicology* 2013; **26 (8)**: 1199-208.
106. Quinn B. Preparation and Maintenance of Live Tissues and Primary Cultures for Toxicity Studies. *Biochemical Ecotoxicology: Principles and Methods* 2014: 33-47.

107. Katt ME, Placone AL, Wong AD, Xu ZS, Searson PC. In Vitro Tumor Models: Advantages, Disadvantages, variables, and Selecting the Right Platform. *Frontiers in Bioengineering and Biotechnology* 2016; **4** 12.
108. Judson R, Kavlock R, Martin M, et al. Perspectives on Validation of High-Throughput Assays Supporting 21st Century Toxicity Testing. *ALTEX* 2013; **30 (1)**: 51-6.
109. Shukla SJ, Huang R, Austin CP, Xia M. Foundation review: The future of toxicity testing: a focus on in vitro methods using a quantitative high-throughput screening platform. *Drug Discovery Today* 2010; **15 (23/24)**: 997-1007.
110. Jozefczuk J, Adjaye J. Chapter Six - Quantitative Real-Time PCR-Based Analysis of Gene Expression. Methods in Enzymology: Elsevier; 2011: 99-109.
111. Takahashi K, Tanabe K, Ohnuki M, et al. Induction of Pluripotent Stem Cells from Adult Human Fibroblasts by Defined Factors. *Cell* 2007; **131**: 861-72.
112. Burridge PW, Thompson S, Millrod MA, et al. A Universal System for Highly Efficient Cardiac Differentiation of Human Induced Pluripotent Stem Cells That Eliminates Interline Variability. *PLoS One* 2011; **6(4)**: e18293.
113. Lian X, Zhang J, Azarin SM, et al. Directed cardiomyocyte differentiation from human pluripotent stem cells by modulating Wnt/β-catenin signaling under fully defined conditions. *Nature Protocols* 2013; **8 (1)**: 162-75.
114. Nicoletti I, Migliorati G, Pagliacci MC, Grignani F, Riccardi C. A rapid and simple method for measuring thymocyte apoptosis by propidium iodide staining and flow cytometry. *Journal of Immunological Methods* 1991; **129**: 271-9.
115. Darzynkiewicz Z, Bruno S, Del Bino G, et al. Features of Apoptotic Cells Measured by Flow Cytometry. *Cytometry* 1992; **13**: 795-808.
116. Scott CW, Zhang X, Abi-Gerges N, Lamore SD, Abassi YA, Peters MF. An Impedance-Based Cellular Assay Using Human iPSC-Derived Cardiomyocytes to Quantify Modulators of Cardiac Contractility. *Toxicological Sciences* 2014; **142 (2)**: 331–8.
117. Nguemo F, Nembo EN, Kamga Kapchoup MV, Enzmann F, Hescheler J. QuinoMit Q10-Fluid attenuates hydrogen peroxide-induced irregular beating in mouse pluripotent stem cell-derived cardiomyocytes. *Biomedicine & Pharmacotherapy* 2021; **142**: 112089.
118. Ndjenda II MK, Nguelefack-Mbuyo EP, Hescheler J, Nguelefack TB, Nguemo F. Assessment of the In Vitro Cytotoxicity Effects of the Leaf Methanol Extract of Crinum zeylanicum on Mouse Induced Pluripotent Stem Cells and Their Cardiomyocytes Derivatives. *Pharmaceuticals* 2021; **14 (12)**: 1208.
119. Chaudhari U, Nemade H, Wagh V, et al. Identification of genomic biomarkers for anthracycline-induced cardiotoxicity in human iPSC-derived cardiomyocytes: an in vitro repeated exposure toxicity approach for safety assessment. *Archives of Toxicology* 2016; **90 (11)**: 2763-77.

120. Stefanowicz-Hajduk J, Ochocka JR. Real-time cell analysis system in cytotoxicity applications: Usefulness and comparison with tetrazolium salt assays. *Toxicology Reports* 2020; **7**: 335-44.
121. Agilent Technologies I. Real-Time and Dynamic Monitoring of Cell Proliferation and Viability for Adherent Cells. 2020. https://www.agilent.com/cs/library/applications/application-cell-proliferation-viability-adherent-cells-xCELLigence-5994-1695en-agilent.pdf (accessed 09/21/ 2022).
122. Xi B, Wang T, Li N, et al. Functional Cardiotoxicity Profiling and Screening Using the xCELLigence RTCA Cardio System. *Journal of Laboratory Automation* 2011; **16 (6)**: 415-21.
123. Accela. xCELLigence Cardio ECR – Agilent technologies. 2024. https://www.accela.eu/agilent-technologies/xcelligence-cardio-ecr (accessed 07/10/ 2024).
124. Ramis G, Martínez-Alarcón L, Quereda JJ, et al. Optimization of cytotoxicity assay by real-time, impedance-based cell analysis. *Biomedical Microdevices* 2013; **15 (6)**: 985-95.
125. Slanina H, König A, Claus H, Frosch M, Schubert-Unkmeir A. Real-time impedance analysis of host cell response to meningococcal infection. *Journal of Microbiological Methods* 2011; **84 (1)**: 101–8.
126. Leme DM, Grummt T, Heinze R, et al. Cytotoxicity of water-soluble fraction from biodiesel and its diesel blends to human cell lines. *Ecotoxicology and Environmental Safety* 2011; **74 (8)**: 2148–55.
127. Keogh R. New technology for investigating trophoblast function. *Placenta* 2010; **31 (4)**: 347–50.
128. Nguemo F, Šaric T, Pfannkuche K, Watzele M, Reppel M, Hescheler J. In vitro Model for Assessing Arrhythmogenic Properties of Drugs Based on High-resolution Impedance Measurements. *Cellular Physiology and Biochemistry* 2012; **29 (5-6)**: 819-32.
129. Stett A, Egert U, Guenther E, et al. Biological application of microelectrode arrays in drug discovery and basic research. *Analytical and Bioanalytical Chemistry* 2003; **377 (3)**: 486-95.
130. Pradhapan P, Kuusela J, Viik J, Aalto-Setälä K, Hyttinen J. Cardiomyocyte MEA Data Analysis (CardioMDA) – A Novel Field Potential Data Analysis Software for Pluripotent Stem Cell Derived Cardiomyocytes. *PLOS ONE* 2013; **8 (9)**: e73637.
131. Berdondini L, Imfeld K, Maccione A, et al. Active pixel sensor array for high spatio-temporal resolution electrophysiological recordings from single cell to large scale neuronal networks†. *Lab on a Chip* 2009; **9 (18)**: 2644-51.

132. Kussauer S, David R, Lemcke H. hiPSCs Derived Cardiac Cells for Drug and Toxicity Screening and Disease Modeling: What Micro-Electrode-Array Analyses Can Tell Us. *Cells* 2019; **8 (11)**: 1331.
133. Pfannkuche K, Liang H, Hannes T, et al. Cardiac myocytes derived from murine reprogrammed fibroblasts: intact hormonal regulation, cardiac ion channel expression and development of contractility. *Cellular Physiology and Biochemistry* 2009; **24 (1-2)**: 73-86.
134. Gonzalez MD, Vassalle M. Electrical and mechanical effects of strontium in sheep cardiac Purkinje fibres. *Cardiovascular Research* 1989; **23 (10)**: 867-81.
135. U.S. Department of Health and human services. Toxicological Profile for Strontium 2004. https://www.atsdr.cdc.gov/toxprofiles/tp159.pdf#:~:text=Int%20J%20Cardiol%2027%3A87,Riera%20A (accessed 06/19/ 2025).
136. Xing M, Jiang Y, Bi W, et al. Strontium ions protect hearts against myocardial ischemia/reperfusion injury. *ScienceAdvances* 2021; **7 (3)**: eabe0726.
137. Hendrych M, Olejnickova V, Novakova M. Calcium versus strontium handling by the heart muscle. *General Physiology and Biophysics* 2016; **35 (1)**: 13-23.
138. R&D Systems. Strontium Chloride. 2025. https://www.rndsystems.com/products/strontium-chloride_4749#:~:text=Biological%20Activity (accessed 06/19/ 2025).
139. Chattopadhyay N, Quinn SJ, Kifor O, Ye C, Brown EM. The calcium-sensing receptor (CaR) is involved in strontium ranelate-induced osteoblast proliferation. *Biochemical Pharmacology* 2007; **74 (3)**: 438-47.
140. Lu F-H, Tian Z, Zhang W-H, et al. Calcium-sensing receptors regulate cardiomyocyte Ca2+ signaling via the sarcoplasmic reticulum-mitochondrion interface during hypoxia/reoxygenation. *Journal of Biomedical Science* 2010; **17 (50)**: 1-11.
141. Giorgi C, Baldassari F, Bononi A, et al. Mitochondrial Ca2+ and apoptosis. *Cell Calcium* 2012; **52 (1)**: 36-43.
142. Kong Y, Guo Y, Zhang J, Zhao B, Wang J. Strontium Promotes Transforming Growth Factors β1 and β2 Expression in Rat Chondrocytes Cultured In Vitro. *Biological Trace Element Research* 2018; **184 (2)**: 450–5.
143. Louis F, Bouleftour W, Rattner A, Linossier M-T, Vico L, Guignandon A. RhoGTPase stimulation is associated with strontium chloride treatment to counter simulated microgravity-induced changes in multipotent cell commitment. *NPJ Microgravity* 2017; **3**: 7.
144. Liu G, Ma C, Yang H, Zhang P-Y. Transforming growth factor β and its role in heart disease. *Experimental And Therapeutic Medicine* 2017; **13 (5)**: 2123-8.

145. Gilbert G, Demydenko K, Dries E, et al. Calcium Signaling in Cardiomyocyte Function. *Cold Spring Harbor Perspectives in Biology* 2020; **12 (3)**: 1035428.
146. Dewenter M, von der Lieth A, Katus HA, Backs J. Calcium Signaling and Transcriptional Regulation in Cardiomyocytes. *Circulation Research* 2017; **121 (8)**: 1000-20.
147. Wu H, Naya FJ, McKinsey TA, et al. MEF2 responds to multiple calcium-regulated signals in the control of skeletal muscle fiber type. *The EMBO Journal* 2000; **19 (9)**: 1963-73.
148. Gao C, Wang Y. A New linc(-RNA) Between NFAT/MEF2 and Cardiac Hypertrophy. *Circulation Research* 2024; **135 (3)**: 450-2.
149. Al-Duliamy MJ, Ghaib NH, Kader OA, Abdullah BH. Enhancement of orthodontic anchorage and retention by the local injection of strontium: An experimental study in rats. *The Saudi Dental Journal* 2015; **27 (1)**: 22-9.
150. Durmuş K, Turgut NH, Doğan M, et al. Histopathological evaluation of the effect of locally administered strontium on healing time in mandibular fractures: An experimental study. *Advances in Clinical and Experimental Medicine* 2017; **26 (7)**: 1063–7.
151. Saad SM, Yasin S, Jain N, LeLorier P. Cardiac Manifestations in a Case of Severe Hyperkalemia. *Cureus* 2021; **13 (3)**: e13641.
152. Ferreira JP, Butler J, Rossignol P, et al. Abnormalities of Potassium in Heart Failure: JACC State-of-the-Art Review. *JACC Journals* 2020; **72 (22): 2836-2850**.
153. Rope K. Complications of High Potassium Levels. 2024. https://www.webmd.com/a-to-z-guides/high-potassium-complications (accessed 06/19/ 2015).
154. Han C-K, Kuo W-W, Shen C-Y, et al. Dilong prevents the high-KCl cardioplegic solution administration-induced apoptosis in H9c2 cardiomyoblast cells mediated by MEK. *The American Journal of Chinese Medicine* 2014; **42 (6)**: 1507-19.
155. Zieschang M. Behandlung der Hyperkaliämie bei Erwachsenen. *Arzneimittelverordnung in der Praxis* 2023; **50 (1)**: 14-29.
156. Vaughan-Jones RD, Spitzer KW, Swietach P. Intracellular pH regulation in heart. *Journal of Molecular and Cellular Cardiology* 2009; **46 (3)**: 318-31.
157. Yost S, Duran-Pinedo AE, Krishnan K, Frias-Lopez J. Potassium is a key signal in host-microbiome dysbiosis in periodontitis. *PLOS Pathogens* 2017; **13 (6)**: e1006457.
158. Sun M, Chen M, Dawood F, et al. Tumor Necrosis Factor-? Mediates Cardiac Remodeling and Ventricular Dysfunction After Pressure Overload State. *Circulation* 2007; **115 (11)**: 398-1407.
159. Schumacher SM, Prasad SVN. Tumor Necrosis Factor-α in Heart Failure: An Updated Review. *Current Cardiology Reports* 2018; **20(11)**: 117.
160. Yasukawa H, Hoshijima M, Gu Y, et al. Suppressor of cytokine signaling-3 is a biomechanical stress–inducible gene that suppresses gp130-mediated cardiac myocyte

hypertrophy and survival pathways. *The Journal of Clinical Investigation* 2001; **108 (10)**: 1459-67.

161. Naima J, Ohta Y. Potassium Ions Decrease Mitochondrial Matrix pH: Implications for ATP Production and Reactive Oxygen Species Generation. *International Journal of Molecular Sciences* 2024; **25 (2)**: 1233.
162. ChemWatch. Potassium Carbonate. 2011. https://datasheets.scbt.com/sc-203206.pdf#:~:text=SWALLOWED%20%21%20Accidental%20ingestion%20of,EYE (accessed 06/19/ 2025).
163. Kaese S, Verheule S. Cardiac electrophysiology in mice: a matter of size. *Frontiers* 2012; **3 (345)**: 1-19.
164. Janssen PML, Biesiadecki BJ, Ziolo MT, Davis JP. The Need for Speed: Mice, Men, and Myocardial Kinetic Reserve. *Circulation Research* 2016; **119 (3)**: 418-21.
165. Ahrens-Nicklas RC, Christini DJ. Anthropomorphizing the Mouse Cardiac Action Potential via a Novel Dynamic Clamp Method. *Biophysical Journal* 2009; **97 (10)**: 2684-92.
166. Deng S, Li C, Chen J, et al. Effects of triclosan exposure on stem cells from human exfoliated deciduous teeth (SHED) fate. *Science of the Total Environment* 2023; **905** 167053.
167. Manzoor Q, Sajid A, Ali Z, et al. Toxicity spectrum and detrimental effects of titanium dioxide nanoparticles as an emerging pollutant: A review. *Desalination and Water Treatment* 2024; **317** 100025.
168. Sarikhani M, Moghaddam SV, Firouzamandi M, et al. Harnessing rat derived model cells to assess the toxicity of TiO2 nanoparticles. *Journal of Materials Science: Materials in Medicine* 2022; **33 (5)**: 41.
169. Zhang X, Song Y, Gong H, et al. Neurotoxicity of Titanium Dioxide Nanoparticles: A Comprehensive Review. *International Journal of Nanomedicine* 2023; **18**: 7183-204.
170. Chuang AH, Bordlemay J, Goodin JL, McPherson III J. Effect of Sodium Lauryl Sulfate (SLS) on Primary Human Gingival Fibroblasts in an In Vitro Wound Healing Model. *Military Medicine* 2019; **184**: 97-101.
171. Ghapanchi J, Kamali F, Moattari A, et al. In Vitro Comparison of Cytotoxic and Antibacterial Effects of 16 Commercial Toothpastes. *Journal of International Oral Health* 2015; **7 (3)**: 39-43.
172. Healy C, Cruchley A, Thornhill M, Williams D. The effect of sodium lauryl sulphate, triclosan and zinc on the permeability of normal oral mucosa. *Oral Diseases* 2000; **6**: 118-23.
173. Herlofson BB, Brodin P, Aars H. Increased human gingival blood flow induced by sodium lauryl sulfate. *Journal of clinical periodontology* 1996; **23**: 1004-7.

174. Tabatabaei MH, Mahounak FS, Asgari N, Moradi Z. Cytotoxicity of the Ingredients of Commonly Used Toothpastes and Mouthwashes on Human Gingival Fibroblasts. *Frontiers in Dentistry* 2019; **16(6)**: 450- 7.
175. Petrović B, Kojić S, Milić L, et al. Toothpaste ingestion—evaluating the problem and ensuring safety: systematic review and meta-analysis. *Frontiers Public Health* 2023; **11**: 1279915.
176. Mani A, Thawani V. Are All Additives of Toothpastes Rational? *Journal of Mahatma Gandhi Institute of Medical Sciences* 2019; **24(2)**: 71.
177. Rode SdM, Sato TdP, Matos FdS, Correia AMdO, Camargo SEA. Toxicity and effect of whitening toothpastes on enamel surface. *Braz Oral Res* 2021; **35**: e025.
178. Saad H, Escoube R, Babajko S, Houari S. Fluoride Intake Through Dental Care Products: A Systematic Review. *Frontiers in Oral Health* 2022; **3**: 916372.
179. Birant S, Duran Y, Akkoc T, Seymen F. Cytotoxic effects of different detergent containing children's toothpastes on human gingival epithelial cells. *BMC Oral Health* 2022; **22**: 66.
180. Kanouté A, Dieng SN, Diop M, et al. Chemical vs. natural toothpaste: which formulas for which properties? A scoping review. *Journal of Public Health in Africa* 2022; **13 (3)**: 1945.

7. Appendix

7.1. List of Figures

7.2. List of Tables

8. Preliminary Publications of Results

Parts of this work have been published in the following article:

Title: Deciphering the Cellular Effects of Strontium Chloride and Potassium Carbonate on Induced Pluripotent Stem Cells and Their Derivative Cardiomyocytes

Journal: Pharmaceuticals, 2026, 19(3), 362; https://doi.org/10.3390/ph19030362